

## Predicting the Structure of Supramolecular Dendrimers via the Analysis of Libraries of AB<sub>3</sub> and Constitutional Isomeric AB<sub>2</sub> Biphenylpropyl Ether Self-Assembling Dendrons

Brad M. Rosen,<sup>†</sup> Daniela A. Wilson,<sup>†</sup> Christopher J. Wilson,<sup>†</sup> Mihai Peterca,<sup>†,‡</sup>  
 Betty C. Won,<sup>†</sup> Chenghong Huang,<sup>†</sup> Linda R. Lipski,<sup>†</sup> Xiangbing Zeng,<sup>§</sup>  
 Goran Ungar,<sup>§</sup> Paul A. Heiney,<sup>‡</sup> and Virgil Percec<sup>\*,†</sup>

Roy & Diana Vagelos Laboratories, Department of Chemistry, University of Pennsylvania, Philadelphia, Pennsylvania 19104-6323, Department of Physics and Astronomy, University of Pennsylvania, Philadelphia, Pennsylvania 19104-6396, and Department of Engineering Materials, University of Sheffield, Sheffield S1 3JD, U.K.

Received September 16, 2009; E-mail: percec@sas.upenn.edu

**Abstract:** The synthesis of 4'-hydroxy-4-biphenylpropionic, 3',4'-dihydroxy-4-biphenylpropionic, 3',5'-dihydroxy-4-biphenylpropionic, and 3',4',5'-trihydroxy-4-biphenylpropionic methyl esters via three efficient and modular strategies including one based on Ni-catalyzed borylation and sequential cross-coupling is reported. These building blocks were employed in a convergent iterative approach to the synthesis of one library of 3,4,5-trisubstituted and two libraries of constitutional isomeric 3,4- and 3,5-disubstituted biphenylpropyl ether dendrons. Structural and retrostructural analysis of supramolecular dendrimers revealed that biphenylpropyl ether dendrons self-assemble and self-organize into the same periodic lattices and quasi-periodic arrays observed in previously reported libraries, but with larger dimensions, different mechanisms of self-assembly, and improved solubility, thermal, acidic, and oxidative stability. The different mechanisms of self-assembly led to the discovery of two new supramolecular structures. The first represents a new banana-like lamellar crystal with a four layer repeat. The second is a giant vesicular sphere self-assembled from 770 dendrons that exhibits an ultrahigh molar mass of  $1.73 \times 10^6$  g/mol. Thus, the enhanced size of the self-assembled structures constructed from biphenylpropyl ether dendrons permitted for the first time discrimination of various molecular mechanisms of spherical self-assembly and elaborated a continuum between small filled spheres and very large hollow spheres that is dictated by the primary structure of the dendron. The comparative analysis of libraries of biphenylpropyl ether dendrons with the previously reported libraries of benzyl-, phenylpropyl-, and biphenyl-4-methyl ether dendrons demonstrated biomimetic self-assembly wherein the primary structure of the dendron and to a lesser extent the structure of its repeat unit determines the supramolecular tertiary structure. A "nanoperiodic table" of self-assembling dendrons and supramolecular dendrimers that allows the prediction of the general features of tertiary structures from primary structures was elaborated.

### Introduction

Dendrons and dendrimers<sup>1</sup> prepared through iterative *convergent*<sup>2</sup> or *divergent*<sup>3</sup> synthesis are perfectly branched molecules that have fostered advances at the interface of chemistry,

biology, physics, medicine, nanoscience, and bionanotechnology. Most dendrons and dendrimers do not self-assemble or self-organize and, therefore, exhibit liquid or amorphous structures. Our laboratory developed strategies for the design of self-assembling *quasi-equivalent* building blocks that mimic the structure and function of complex biological systems through the strategic combination of chemically dissimilar units in the structure of the dendron. Benzyl ether dendrons functionalized with aliphatic or semifluorinated alkyl groups are examples that mediate self-assembly into a variety of periodic lattices and quasi-periodic arrays.<sup>4</sup> Additional approaches to self-assembling dendrons and related structures by merging chemically dissimilar

<sup>†</sup> Department of Chemistry.

<sup>‡</sup> Department of Physics and Astronomy.

<sup>§</sup> University of Sheffield.

- (1) (a) Fréchet, J. M. J.; Tomalia, D. A., Eds. *Dendrimers and Other Dendritic Polymers*; Wiley: New York, 2001. (b) Newkome, G. R.; Moorefield, C. N.; Vögtle, F. *Dendrimers and Dendrons*; Wiley-VCH: Weinheim, 2001. (c) Vögtle, F.; Richardt, G.; Werner, N. *Dendrimer Chemistry*; Wiley-VCH: Weinheim, 2009.
- (2) (a) Buhleier, E.; Wehner, W.; Vögtle, F. *Synthesis* **1978**, 155–158. (b) Tomalia, D. A.; Baker, H.; Dewald, J.; Hall, M.; Kallos, G.; Martin, S.; Roeck, J.; Ryder, J.; Smith, P. *Polym. J.* **1985**, *17*, 117–132. (c) Newkome, G. R.; Yao, Z.; Baker, G. R.; Gupta, V. K. *J. Org. Chem.* **1985**, *50*, 2003–2004.
- (3) (a) Hawker, C. J.; Fréchet, J. M. J. *J. Am. Chem. Soc.* **1990**, *112*, 7638–7647. (b) Miller, T. M.; Neenan, T. X. *Chem. Mater.* **1990**, *2*, 346–349. (c) Grayson, S. M.; Fréchet, J. M. J. *Chem. Rev.* **2001**, *101*, 3819–3868.

- (4) (a) Balagurusamy, V. S. K.; Ungar, G.; Percec, V.; Johansson, G. *J. Am. Chem. Soc.* **1997**, *119*, 1539–1555. (b) Percec, V.; Cho, W.-D.; Ungar, G.; Yeardeley, D. J. P. *J. Am. Chem. Soc.* **2001**, *123*, 1302–1315. (c) Percec, V.; Mitchell, C. M.; Cho, W.-D.; Uchida, S.; Glodde, M.; Ungar, G.; Zeng, X.; Liu, Y.; Balagurusamy, V. S. K.; Heiney, P. A. *J. Am. Chem. Soc.* **2004**, *126*, 6078–6094.

subunits were elaborated by other laboratories.<sup>5</sup> Our laboratory generated methods for the structural and retrostructural analysis of the *p6mm* hexagonal columnar ( $\Phi_h$ ), *p2mm* simple rectangular columnar ( $\Phi_{r-s}$ ), and the *c2mm* centered rectangular columnar ( $\Phi_{r-c}$ ) periodic lattices to determine the conformation of the dendrons during self-assembly.<sup>4b</sup> Subsequently, the first spherical supramolecular dendrimers that self-organize into cubic *Pm $\bar{3}n$*  (*Cub*),<sup>4a</sup> cubic *Im $\bar{3}m$*  (*BCC*),<sup>4b,6</sup> tetragonal *P4<sub>2</sub>/mmm* (*Tet*) lattices<sup>7</sup> and into 12-fold quasi-liquid crystalline (*QLC*) arrays<sup>8</sup> were discovered, and methods for their retrostructural analysis were elaborated. Originally, columnar and spherical supramolecular dendrimers were considered to be micellar. However, adaptation of Cochran, Crick, and Vand helical diffraction theory<sup>9</sup> to incorporate tilted groups of atoms revealed features that demonstrated internal helical order in the supramolecular columns<sup>10</sup> derived from self-assembling dendrons and dendrimers. Recently, it was discovered that supramolecular spheres can be chiral<sup>11</sup> or chiral hollow,<sup>12</sup> which brought into question the micellar structure of spherical dendrimers. In addition to providing insight into the mechanisms of self-assembly in biological and synthetic systems, the internal structures of supramolecular dendrimers generated from aryl ether dendrons and dendrimers have been exploited for the design of complex systems such as self-repairing supramolecular electronic materials,<sup>13</sup> porous protein mimics,<sup>14</sup> supramolecular containers,<sup>12</sup> thixotropic gels,<sup>15</sup> and nanomechanical actuators.<sup>16</sup>

Through the synthesis as well as structural and retrostructural analysis of libraries of AB<sub>2</sub>,<sup>4b</sup> AB<sub>3</sub>,<sup>4b</sup> AB<sub>4</sub>,<sup>17</sup> AB<sub>5</sub>,<sup>17</sup> and AB<sub>y</sub>-AB<sub>n</sub><sup>4c</sup> self-assembling benzyl ether dendrons, it was discovered that the primary structure of the dendron determines the tertiary structure of the resulting supramolecular dendrimers, their quaternary structure (self-organized periodic lattice or quasi-periodic array), and the mechanism of self-assembly. The structural and retrostructural analysis of a library of phenylpropyl ether dendrons<sup>18</sup> that are more flexible than the corresponding benzyl ether dendrons<sup>4</sup> proved that self-assembly is also possible with dendritic building blocks which access conformations similar to the *trans* and *gauche* conformations of the benzyl ethers building blocks. Benzyl ether dendrons provided the most investigated class of self-assembling and self-organizable dendrons.<sup>4</sup> However, they exhibit acidic and oxidative instability, and their corresponding supramolecular dendrimers are limited in size. In addition, the structural and retrostructural analysis of libraries of phenylpropyl<sup>18</sup> and biphenyl-4-methyl ether dendrons<sup>19</sup> demonstrated the tolerance of the self-assembly process to larger dendritic building blocks and provided access to larger supramolecular structures. However, phenylpropyl ether dendrons exhibit low phase transitions, although they are more stable under acidic conditions than benzyl ether dendrons. In addition, the phenolates derived from phenylpropyl ether building blocks are oxidatively less stable than those derived from benzyl ethers. While the biphenyl-4-methyl ether building blocks exhibited enhanced stability to oxidation, biphenyl-4-methyl ether dendrons were less soluble, thereby restricting the size of the library that could be synthesized and analyzed.

Herein, the synthesis as well as structural and retrostructural analysis of a new class of self-assembling biphenylpropyl (BpPr) ether dendrons is reported. The BpPr building block was constructed to synergistically combine the size of phenylpropyl and biphenyl-4-methyl ether dendrons with the most desirable combination of solubility and acidic and oxidative stability. New supramolecular structures discovered during the synthesis of the libraries of BpPr dendrons are also presented. BpPr dendrons were designed to facilitate comparison of all previously reported libraries of self-assembling aryl ether dendrons. This compar-

- (5) For select examples of other approaches to self-assembling dendrons based on the combination of chemical dissimilar subunits, see: (a) Zubarev, E. R.; Pralle, M. U.; Sone, E. D.; Stupp, S. I. *J. Am. Chem. Soc.* **2001**, *123*, 4105–4106. (b) Kato, T. *Science* **2002**, *295*, 2414–2418. (c) Liang, C. O.; Helms, B.; Hawker, C. J.; Fréchet, J. M. J. *Chem. Commun.* **2003**, 2524–2525. (d) Yoo, Y.-S.; Choi, J.-H.; Song, J. H.; Oh, N.-K.; Zin, W.-C.; Park, S.; Chang, T.; Lee, M. *J. Am. Chem. Soc.* **2004**, *126*, 6294–6300. (e) Ryu, J.-H.; Bae, J.; Lee, M. *Macromolecules* **2005**, *38*, 2050–2052. (f) Zeng, X.; Impéror-Clerc, M. *Nat. Mater.* **2005**, *4*, 562–567. (g) Kim, J. K.; Hong, M. K.; Ahn, J. H.; Lee, M. *Angew. Chem., Int. Ed.* **2005**, *44*, 328–332. (h) Bae, J.; Choi, J.-H.; Oh, N.-K.; Kim, B.-S.; Lee, M. *J. Am. Chem. Soc.* **2005**, *127*, 9668–9669. (i) Cho, B. K.; Jain, A.; Gruner, S. M.; Wiesner, U. *Chem. Commun.* **2005**, 2143–2145. (j) Park, C.; Choi, K. S.; Song, Y.; Jeon, H. J.; Song, H. H.; Chang, J. Y.; Kim, C. *Langmuir* **2006**, *22*, 3812. (k) Sakai, N.; Kamikawa, Y.; Nishii, M.; Matsuoka, T.; Kato, T.; Matile, S. *J. Am. Chem. Soc.* **2006**, *128*, 2218–2219. (l) Ryu, J. H.; Kim, H. J.; Huang, Z. G.; Lee, E.; Lee, M. *Angew. Chem., Int. Ed.* **2006**, *45*, 5304–5307. (m) Zhang, X.; Chen, Z.; Würthner, F. *J. Am. Chem. Soc.* **2007**, *129*, 4886–4887. (n) Li, B.; Martin, A. L.; Gillies, E. R. *Chem. Commun.* **2007**, 5217–5219. (o) Ryu, J.-H.; Lee, E.; Lim, Y.-B.; Lee, M. *J. Am. Chem. Soc.* **2007**, *129*, 4808–4814. (p) Park, C.; Lim, J.; Yun, M.; Kim, C. *Angew. Chem., Int. Ed.* **2008**, *47*, 2959–2969. (q) Li, W.; Zhang, A.; Feldman, K.; Walde, P.; Schlüter, D. A. *Macromolecules* **2008**, *41*, 3659–3667. (r) Sagara, Y.; Kato, T. *Angew. Chem., Int. Ed.* **2008**, *47*, 5175–5178. (s) Lehmann, M.; Jahr, M. *Chem. Mater.* **2008**, *20*, 5453–5456. (t) Miyajima, D.; Tashiro, K.; Araoka, F.; Takazoe, H.; Kim, J.; Kato, K.; Takata, M.; Aida, T. *J. Am. Chem. Soc.* **2009**, *131*, 44–45. (6) Yeardley, D. J. P.; Ungar, G.; Percec, V.; Holerca, M. N.; Johansson, G. *J. Am. Chem. Soc.* **2000**, *122*, 1684–1689. (7) Ungar, G.; Liu, Y.; Zeng, X.; Percec, V.; Cho, W.-D. *Science* **2003**, *299*, 1208–1211. (8) Zeng, X.; Ungar, G.; Liu, Y.; Percec, V.; Dulcey, A. E.; Hobbs, J. K. *Nature* **2004**, *428*, 157–160. (9) Cochran, W.; Crick, F. H. C.; Vand, V. *Acta Crystallogr.* **1952**, *5*, 581–586. (10) Peterca, M.; Percec, V.; Imam, M. R.; Leowanawat, P.; Morimitsu, K.; Heiney, P. A. *J. Am. Chem. Soc.* **2008**, *130*, 14840–14852. (11) Percec, V.; Imam, M. R.; Peterca, M.; Wilson, D. A.; Heiney, P. A. *J. Am. Chem. Soc.* **2009**, *131*, 1294–1304. (12) Percec, V.; Peterca, M.; Dulcey, A. E.; Imam, M. R.; Hudson, S. D.; Nummelin, S.; Adelman, P.; Heiney, P. A. *J. Am. Chem. Soc.* **2008**, *130*, 13079–13094.

- (13) (a) Glodde, M.; Bera, T. K.; Miura, Y.; Shiyonovskaya, I.; Singer, K. D.; Balagurusamy, V. S. K.; Heiney, P. A.; Schnell, I.; Rapp, A.; Spiess, H.-W.; Hudson, S. D.; Duan, H. *Nature* **2002**, *417*, 384–387. (b) Percec, V.; Aqad, E.; Peterca, M.; Imam, M. R.; Glodde, M.; Bera, T. K.; Miura, Y.; Balagurusamy, V. S. K.; Ewbank, P. C.; Würthner, F.; Heiney, P. A. *Chem.—Eur. J.* **2007**, *13*, 3330–3345. (14) (a) Percec, V.; Dulcey, A. E.; Balagurusamy, V. S. K.; Miura, Y.; Smidrkal, J.; Peterca, M.; Nummelin, S.; Hudson, S. D.; Heiney, P. A.; Duan, H.; Magonov, S. N.; Vinogradov, S. A. *Nature* **2004**, *430*, 764–769. (b) Percec, V.; Dulcey, A. E.; Peterca, M.; Iliés, M.; Nummelin, S.; Sienkowska, M. J.; Heiney, P. A. *Proc. Natl. Acad. Sci. U.S.A.* **2006**, *103*, 2518–2523. (c) Percec, V.; Dulcey, A. E.; Peterca, M.; Adelman, P.; Samant, R.; Balagurusamy, V. S. K.; Heiney, P. A. *J. Am. Chem. Soc.* **2007**, *129*, 5992–6002. (15) Percec, V.; Peterca, M.; Yurchenko, M. E.; Rudick, J. G.; Heiney, P. A. *Chem.—Eur. J.* **2007**, *14*, 909–918. (a) Percec, V.; Rudick, J. G.; Peterca, M.; Heiney, P. A. *J. Am. Chem. Soc.* **2008**, *130*, 7503–7508. (16) Rudick, J. G.; Percec, V. *Acc. Chem. Res.* **2008**, *41*, 1641–1652. (17) Percec, V.; Won, B. C.; Peterca, M.; Heiney, P. A. *J. Am. Chem. Soc.* **2007**, *129*, 11265–11278. (18) Percec, V.; Peterca, M.; Sienkowska, M. J.; Iliés, M. A.; Aqad, E.; Smidrkal, J.; Heiney, P. A. *J. Am. Chem. Soc.* **2006**, *128*, 3324–3334. (19) (a) Percec, V.; Holerca, M. N.; Nummelin, S.; Morrison, J. J.; Glodde, M.; Smidrkal, J.; Peterca, M.; Rosen, B. M.; Uchida, S.; Balagurusamy, V. S. K.; Sienkowska, M. J.; Heiney, P. A. *Chem.—Eur. J.* **2006**, *12*, 6216–6241. (b) Percec, V.; Smidrkal, J.; Peterca, M.; Mitchell, C. M.; Nummelin, S.; Dulcey, A. E.; Sienkowska, M.; Heiney, P. A. *Chem.—Eur. J.* **2007**, *13*, 3989–4007.

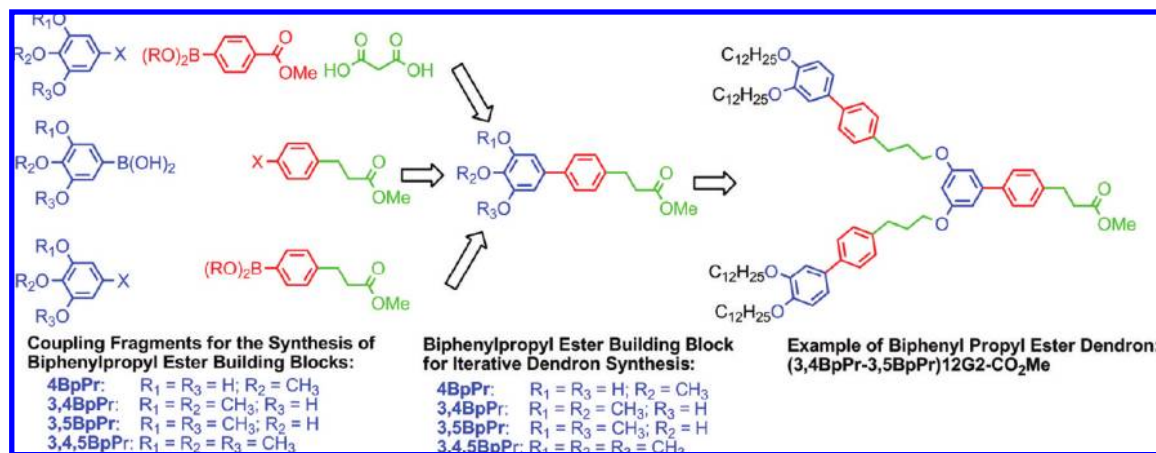


Figure 1. Three modular approaches to BpPr building blocks.

tive analysis provided a “nanoperiodic table”<sup>20</sup> of self-assembling dendrons allowing for the prediction of the structure of the corresponding supramolecular dendrimers.

## Results and Discussion

**Modular Synthesis of Dendritic Building Blocks.** Three modular approaches for the synthesis of 4'-hydroxy-4-biphenylpropionic, 3',4'-dihydroxy-4-biphenylpropionic, 3',5'-dihydroxy-4-biphenylpropionic, and 3',4',5'-trihydroxy-4-biphenylpropionic methyl esters that will subsequently be used in the iterative synthesis of self-assembling BpPr dendrons were elaborated (Figure 1). In previous publications, phenylpropyl ether<sup>18</sup> and biphenyl-4-methyl ether<sup>19a</sup> dendritic building blocks were assigned the short notations Pr and Bp, respectively. Biphenylpropyl ether building blocks are a combination of Pr and Bp structures, and the short notation that will be used for them is BpPr. The three modular approaches outlined in Figure 1 will allow for additional modifications to the structure of the dendritic building block without the need of new synthetic methods. In all three approaches, phenyl-methyl ether and propionic methyl ester groups were selected for the periphery and apex connection points, respectively. These groups were transformed into phenol and propanol groups under orthogonal conditions, as required for their use in *convergent* iterative dendron synthesis.<sup>4,18</sup>

The 3-phenylpropionate building blocks reported previously for the synthesis of Pr dendrons<sup>18</sup> were prepared by Knoevenagel condensation<sup>21</sup> of 4-hydroxy-, 3,4-benzyloxy-, 3,5-benzyloxy-, or 3,4,5-tribenzyloxybenzaldehyde with malonic acid. The biphenyl-4-methyl ether building blocks<sup>19</sup> employed in the synthesis of Bp dendrons were prepared through efficient Ni-catalyzed Suzuki cross-coupling.<sup>22</sup> A three-component synthesis (aryl halide, arylboronic acid, and malonic acid) of BpPr dendritic building blocks (Figure 1 top) was accessible through the direct application of the approaches utilized for Pr and Bp dendrons (Scheme 1). 4-Bromotoluene (**1**) was converted to the

corresponding aryl Grignard reagent, which was trapped with B(OMe)<sub>3</sub>. Acidic hydrolysis provided 4-toluene boronic acid (**2**) in 80% yield after recrystallization from H<sub>2</sub>O. Oxidation of the benzylic carbon with KMnO<sub>4</sub>, followed by esterification in acidic methanol, provided<sup>17</sup> 4-methoxycarbonylphenyl-1-boronic acid (**3**) in 60% yield over two steps. 4-Methoxycarbonyl-1-phenyl boronic acid (**3**) was cross-coupled with 3,4-dimethoxy- or 3,4,5-trimethoxy-1-bromobenzene (**4b,d**) using NiCl<sub>2</sub>(dppe)/dppe<sup>22a</sup> as catalyst to produce the corresponding biphenyl-4-methyl esters (**5**) in 65–75% yield after column chromatography. It is expected that 4-methoxy- and 3,5-dimethoxy-1-bromobenzene (**4a,c**) will also be compatible with this approach.<sup>18,19</sup> The branched biphenyl-4-methyl esters were reduced to their corresponding alcohols (**6**) with LiAlH<sub>4</sub> in 90–95% yield. Reoxidation to the aldehyde (**7**) followed by Knoevenagel condensation with malonic acid gave the branched 4-phenylcinnamic acids (**8**) in 95–100% yield over two steps. Esterification in acidic methanol followed by hydrogenation at atmospheric pressure over Pd/C furnished the BpPr dendritic building blocks **10b,d** in 87–94% yield over two steps. This strategy involves 9 steps and is not suitable for the expeditious synthesis of BpPr dendrons. Nevertheless, the 9 step, three-component approach from Scheme 1 provides maximum flexibility for the modular synthesis of analogous BpPr dendrons through the selection of diversely substituted aryl boronic acids and aryl halides or via Michael addition to the  $\beta$ -unsaturated ester derived from Knoevenagel condensation.

A more rapid approach to the synthesis of BpPr dendritic building blocks relies on commercially available hydrocinnamic acid (**11**) as a C<sub>6</sub>C<sub>3</sub> skeleton for the right-hand piece of the BpPr building block (Figure 1 middle, and Scheme 2). Hydrocinnamic acid (**11**) was directly *para*-iodinated with I<sub>2</sub> in the presence of periodic acid to give 4-iodohydrocinnamic acid (**12**) in 59% yield after recrystallization.<sup>23</sup> Refluxing **12** in acidic methanol provided methyl 4-iodohydrocinnamate (**13**) in nearly quantitative yield (99%).<sup>24a</sup> 4-Methoxy- and 3,4-dimethoxy-1-bromobenzene (**4a,b**) were prepared from anisole and veratrole in 94% and 97% yield, respectively, via treatment with NH<sub>4</sub>Br/

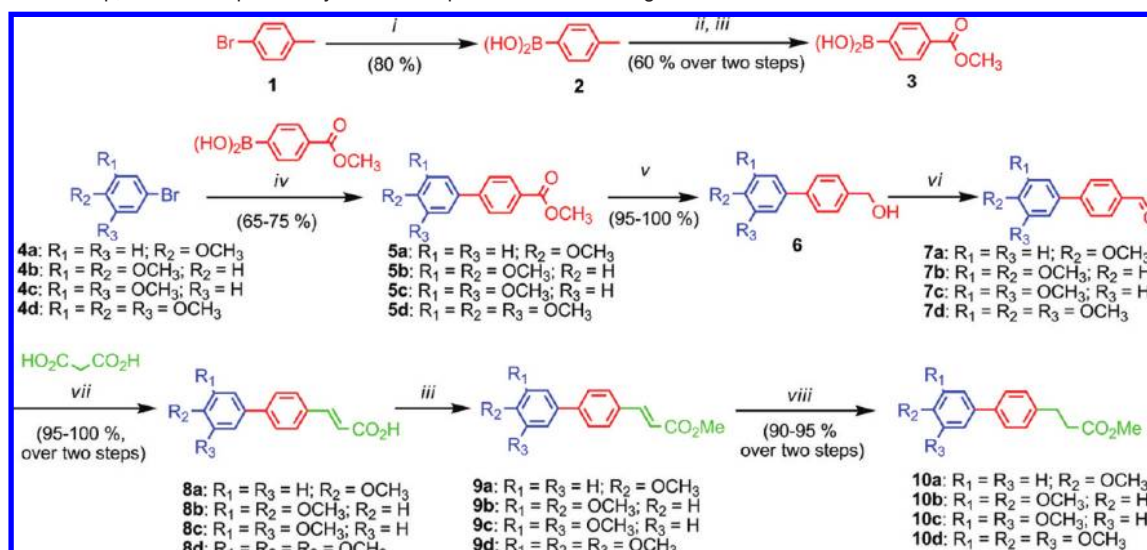
(20) Tomalia, D. A. *J. Nanoparticle Res.* **2009**, *11*, 1251–1310.

(21) Jones, G. *Organic Reactions*; Wiley: New York, 1967; Vol. 15, pp 204–599.

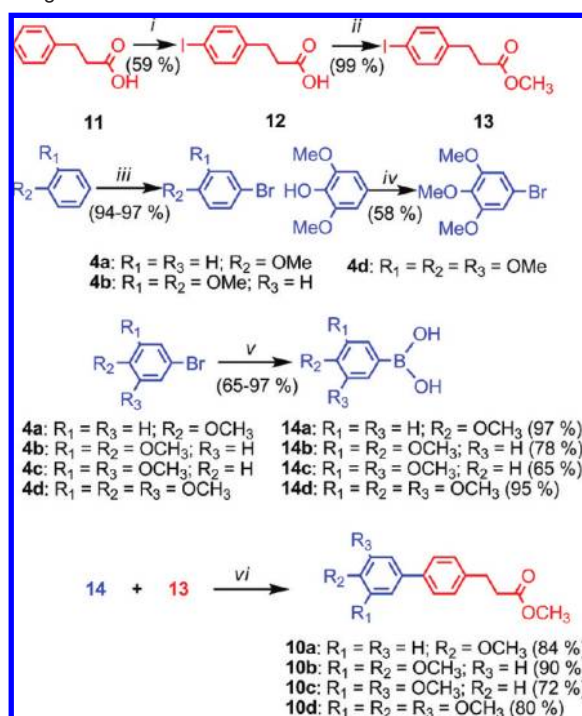
(22) (a) Percec, V.; Golding, G. M.; Smidrkal, J.; Weichold, O. *J. Org. Chem.* **2004**, *69*, 3447–3452. (b) Percec, V.; Bae, J.-Y.; Zhao, M.; Hill, D. H. *J. Org. Chem.* **1995**, *60*, 176–185. (c) Percec, V.; Bae, J.-Y.; Hill, D. H. *J. Org. Chem.* **1995**, *60*, 1060–1065. (d) Percec, V.; Bae, J.-Y.; Zhao, M.; Hill, D. H. *J. Org. Chem.* **1995**, *60*, 1066–1069. (e) Percec, V.; Bae, J.-Y.; Hill, D. H. *J. Org. Chem.* **1995**, *60*, 6895–6903.

(23) Kawasaki, M.; Goto, M.; Kawabata, S.; Kometani, T. *Tetrahedron: Asymmetry* **2001**, *12*, 585–596.

(24) (a) Rosen, B. M.; Huang, C.; Percec, V. *Org. Lett.* **2008**, *10*, 2597–2600. (b) Wilson, D. A.; Wilson, C. J.; Rosen, B. M.; Percec, V. *Org. Lett.* **2008**, *10*, 4879–4882. (c) Moldoveanu, C.; Wilson, D. A.; Wilson, C. J.; Corcoran, P.; Rosen, B. M.; Percec, V. *Org. Lett.* **2009**, *11*, 4974–4977.

**Scheme 1.** Nine Step, Three Component Synthesis of BpPr Dendritic Building Blocks<sup>a</sup>

<sup>a</sup> Reagent and conditions: (i) Mg, I<sub>2</sub>, B(OMe)<sub>3</sub>, THF; (ii) KMnO<sub>4</sub>, H<sub>2</sub>O; (iii) H<sub>2</sub>SO<sub>4</sub>, MeOH; (iv) NiCl<sub>2</sub>(dppe)/dppe, K<sub>3</sub>PO<sub>4</sub>, dioxane; (v) LiAlH<sub>4</sub>, THF; (vi) PCC, CH<sub>2</sub>Cl<sub>2</sub>; (vii) morpholine, AcOH; (viii) H<sub>2</sub>, Pd/C, EtOH.

**Scheme 2.** Improved Four Step Synthesis of BpPr Dendritic Building Blocks<sup>a</sup>

<sup>a</sup> Reagents and conditions: (i) I<sub>2</sub>/H<sub>5</sub>IO<sub>6</sub>, H<sub>2</sub>SO<sub>4</sub>/H<sub>2</sub>O/CH<sub>3</sub>CO<sub>2</sub>H (70 °C); (ii) H<sub>2</sub>SO<sub>4</sub> cat./MeOH (70 °C); (iii) NH<sub>4</sub>Br, H<sub>2</sub>O<sub>2</sub>, AcOH; (iv) (a) NBS, NaH, CHCl<sub>3</sub>; (b) Me<sub>2</sub>SO<sub>4</sub>, K<sub>2</sub>CO<sub>3</sub>, Acetone; (v) Mg (reflux), THF, B(OMe)<sub>3</sub> (-10 °C) or *n*-BuLi, B(OMe)<sub>3</sub> (-78 °C), THF; (vi) 10 mol % Ni(dppe)Cl<sub>2</sub>, 10–15 mol % dppe or 20 mol % PPh<sub>3</sub>, K<sub>3</sub>PO<sub>4</sub>, Dioxane (120 °C).

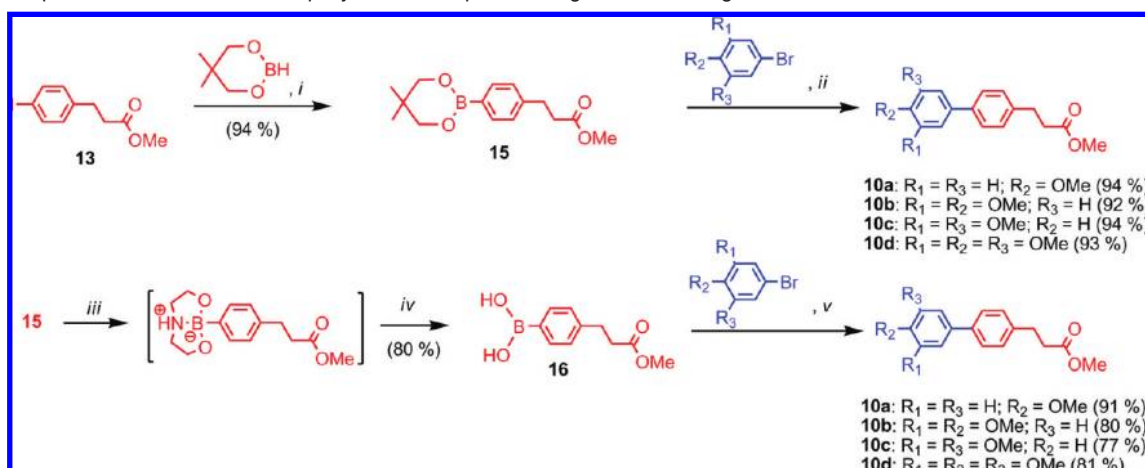
H<sub>2</sub>O<sub>2</sub> in CH<sub>3</sub>COOH.<sup>25</sup> 3,5-Dimethoxy-1-bromobenzene was prepared from commercial sources. 2,6-Dimethoxyphenol was deprotonated with NaH in a mixture of CHCl<sub>3</sub> and MeOH and brominated with *N*-bromosuccinimide (NBS),<sup>26</sup> followed by

methylation with Me<sub>2</sub>SO<sub>4</sub> in acetone to produce 3,4,5-trimethoxy-1-bromobenzene (58%). 4-Methoxy-, 3,4-dimethoxy-, 3,5-dimethoxy-, or 3,4,5-trimethoxyphenyl-1-boronic acids (**14a,b,c,d**) were prepared from the corresponding aryl bromides in 65–97% yield via aryl Grignard or lithium approaches. The synthesis of 3,5-dimethoxyphenyl-1-boronic acid resulted in the lowest yield (65%), while the highest yield (97%) was obtained for the synthesis of 4-methoxyphenyl-1-boronic acid. Methyl 4-iodohydrocinnamate was employed in an efficient and cost-effective NiCl<sub>2</sub>(dppe)-catalyzed Suzuki cross-coupling<sup>22a</sup> with boronic acids **14a,b,c,d** in 72–88% yield. Cross-coupling of **13** with **14a** was accomplished with the mixed-ligand system containing 10 mol % NiCl<sub>2</sub>(dppe) and 20 mol % PPh<sub>3</sub>.<sup>17,22a,24c</sup> Higher yields for the cross-coupling of **13** with **14b** or **14c** were achieved using 10 mol % dppe as coligand. The use of this bidentate dppe coligand inhibited aryl–aryl transfer with the ligand. The 4 step, two-component approach to the synthesis of BpPr dendritic building blocks from Scheme 2 is more rapid than the 9 step, three-component approach from Scheme 1 but is restricted to accessible 4-halocinnamates and branched boronic acids and thus limits the diversity of analogues that can be prepared.

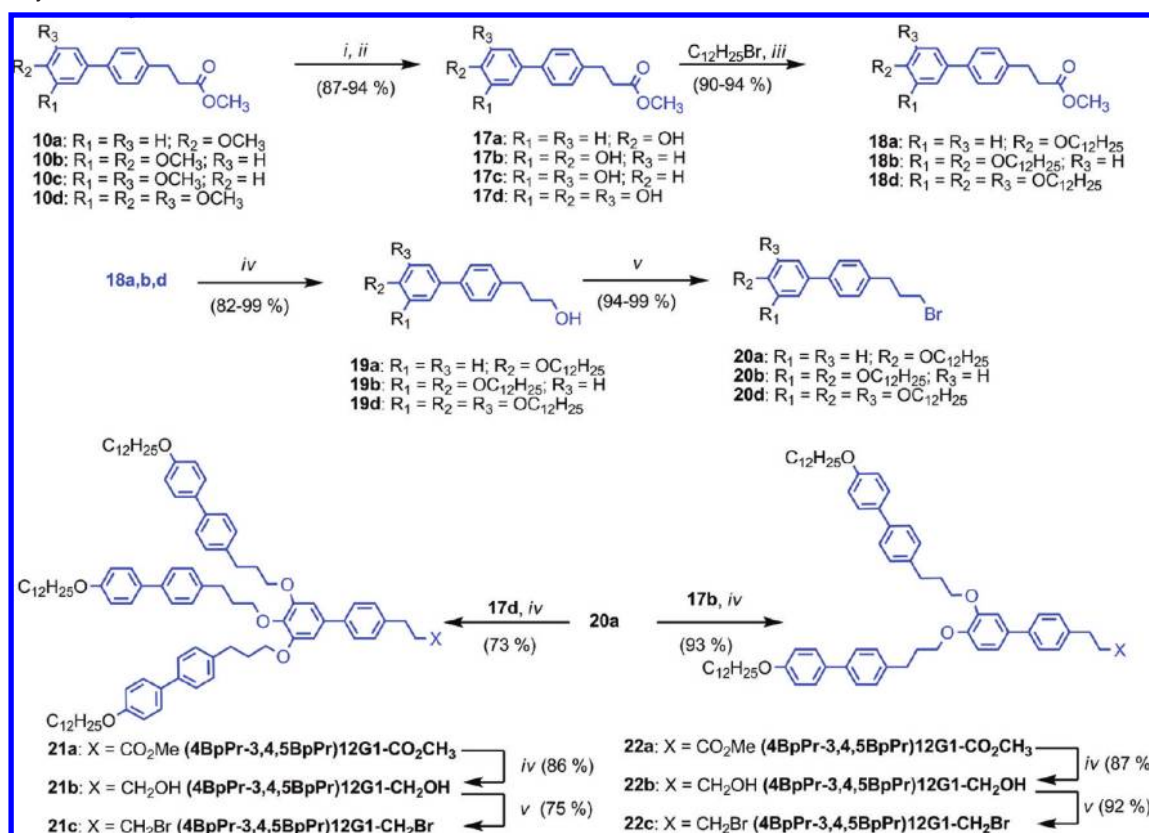
The preparation of four different branched boronic acids was a synthetic bottleneck. Thus, a more expeditious route to the synthesis of BpPr building blocks would involve the cross-coupling of a single hydrocinnamate derived boronic acid or ester with methoxy-substituted aryl halides (Figure 1, bottom). Traditional approaches to the synthesis of boronic acids and esters employ hard metalation conditions which are not tolerated by sensitive electrophilic functionalities, such as the ester in methyl 4-iodohydrocinnamate. Recently, we elaborated an efficient and mild Ni-catalyzed neopentylglycolborylation<sup>24</sup> of aryl bromides, iodides, and chlorides and sequential Ni-catalyzed<sup>24a</sup> or complementary Pd-catalyzed cross-coupling.<sup>24b</sup> Treatment of **13** with 2.0 equiv of in situ prepared neopentylglycolborane (5,5-dimethyl-1,3,2-dioxaborinane) in the presence of 2 mol % Ni(dppp)Cl<sub>2</sub>, 2 mol % dppp coligand, and 3.0 equiv of Et<sub>3</sub>N provided arylneopentylglycolboronate ester **15** in 94% yield after column chromatography (Scheme 3, top). Pd(dppe)Cl<sub>2</sub>-catalyzed Suzuki cross-coupling of **15** with **4a,b,c,d**

(25) Mohan, K. V. V. K.; Narender, N.; Srinivasu, P.; Kulkarni, S. J.; Raghavan, K. V. *Synth. Commun.* **2004**, *34*, 2143–2152.

(26) Foley, J. W. *Chem. Abstr.* **1980**, *92*, 163705x (Synthesis (Polaroid Corp.), US-4182912).

**Scheme 3.** Expedient Four and Five Step Synthesis of BpPr Building Blocks Utilizing One Boronic Acid<sup>a</sup>

<sup>a</sup> Reagents and conditions: (i) 2 mol % NiCl<sub>2</sub> (dppp), 2 mol % dppp, Et<sub>3</sub>N, Toluene (100 °C); (ii) 10 mol % Pd (dppf)Cl<sub>2</sub>, K<sub>3</sub>PO<sub>4</sub>, Dioxane (110 °C); (iii) diethanolamine, *i*PrOH; (iv) 10% H<sub>2</sub>SO<sub>4</sub>, Et<sub>2</sub>O (v) 10 mol % Ni(dppe)Cl<sub>2</sub>, 10 mol % dppe, K<sub>3</sub>PO<sub>4</sub>, Dioxane (120 °C).

**Scheme 4.** Synthesis of First Generation Dendrons<sup>a</sup>

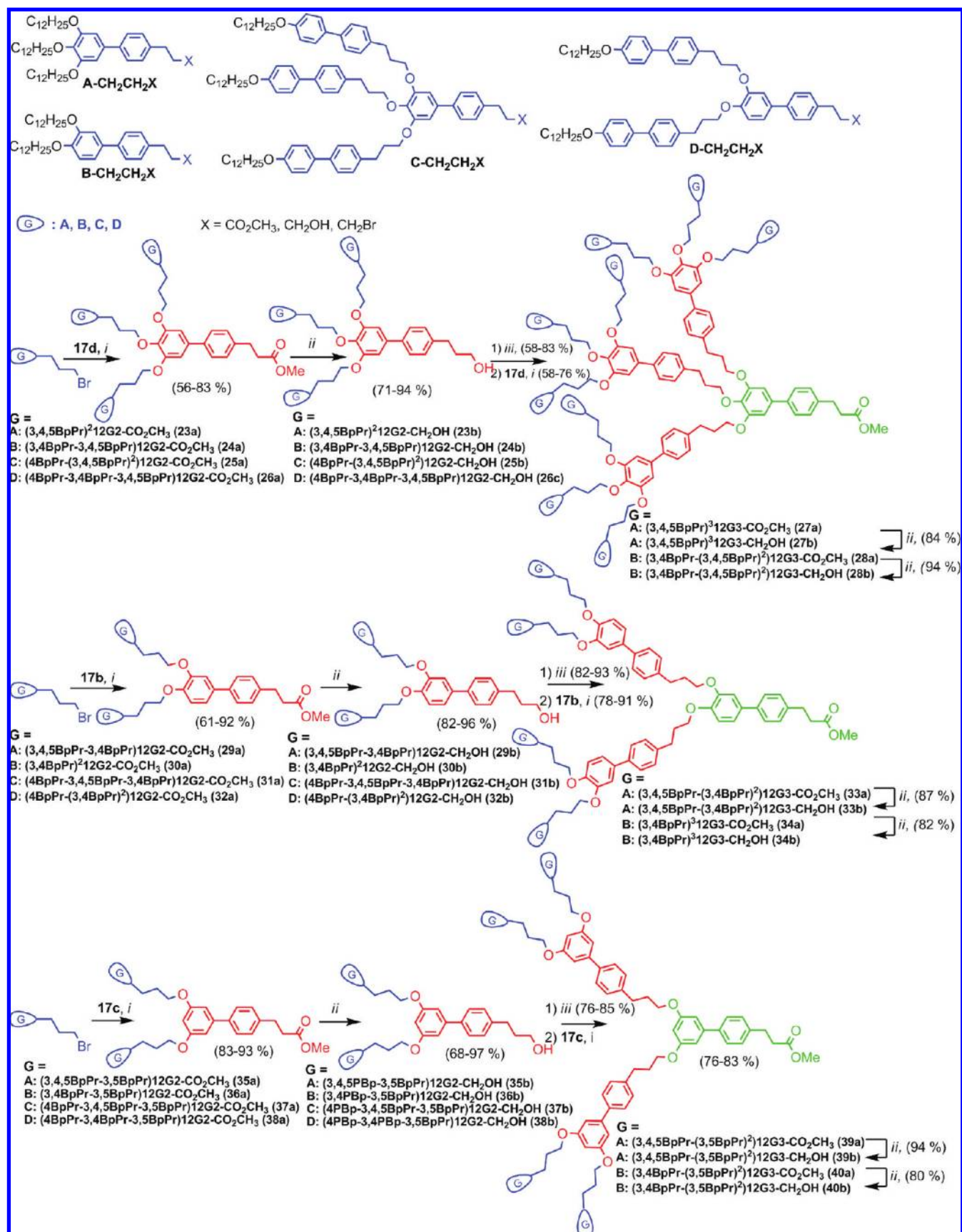
<sup>a</sup> Reagents and conditions: (i) 48% w/w HBr/H<sub>2</sub>O, CH<sub>3</sub>COOH (125 °C); (ii) H<sub>2</sub>SO<sub>4</sub> (cat.), MeOH (75 °C); (iii) K<sub>2</sub>CO<sub>3</sub>, DMF (90–120 °C); (iv) LiAlH<sub>4</sub>, THF, (0–25 °C); (v) NBS, PPh<sub>3</sub>, THF.

provided BpPr building blocks in 92–94% yield after column chromatography. Alternatively, **15** was transesterified with diethanolamine and selectively hydrolyzed to the boronic acid **16**, leaving the sensitive methyl ester intact (Scheme 3, bottom).<sup>27</sup> Ni(dppe)Cl<sub>2</sub>-catalyzed cross-coupling of **18** with aryl bromides **4a,b,c,d** provided BpPr building blocks in 77–89% yield with no evidence of aryl–aryl transfer side reactions. The sequential Ni-catalyzed and complementary Ni/Pd-catalyzed

syntheses are the most rapid for the preparation of BpPr dendritic building blocks as they rely on a single conserved boronic acid that can be coupled with a diversity of commercially available aryl bromides.

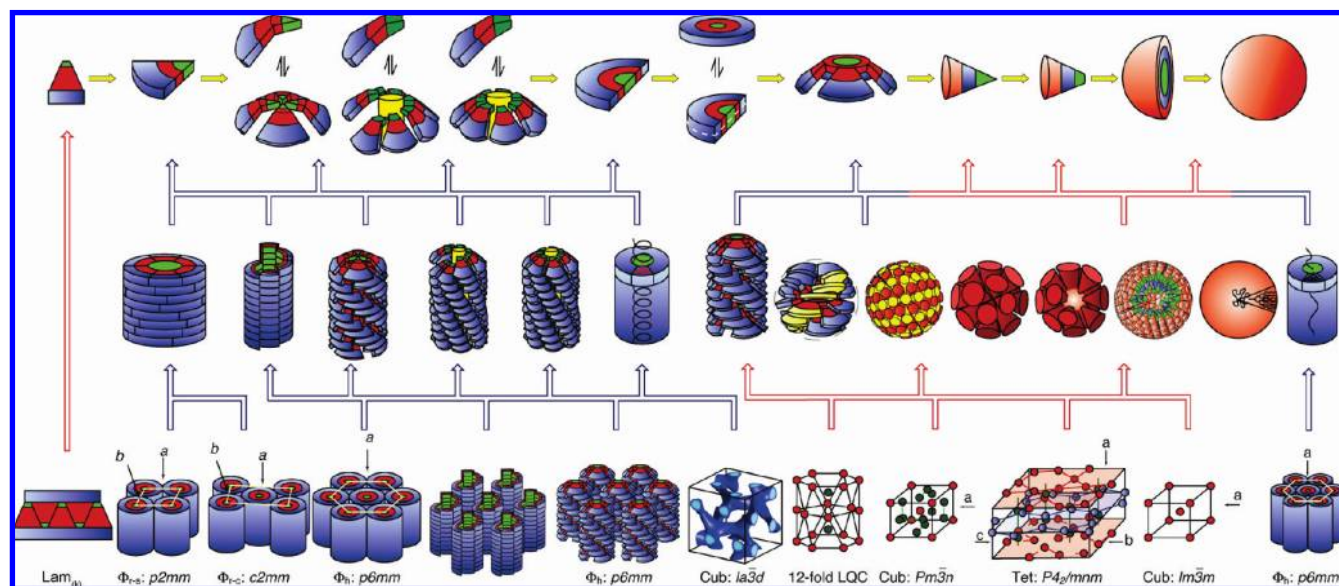
**Synthesis of First-Generation Dendrons.** The synthesis of first (Scheme 4) and higher (Scheme 5) generation dendrons follows an iterative strategy adapted from methods employed for phenylpropyl ether dendrons.<sup>18</sup> BpPr building blocks were converted from their methoxy-protected **10a,b,c,d** to their hydroxy-substituted derivatives **17a,b,c,d** via hydrolysis with 48%

(27) Tripathy, P. B.; Matteson, D. S. *Synthesis* **1989**, 200–206.

Scheme 5. Synthesis of Higher-Generation Dendrons<sup>a</sup>

<sup>a</sup> Reagents and conditions: (i) K<sub>2</sub>CO<sub>3</sub>, DMF, 70 °C; (ii) LiAlH<sub>4</sub>, THF; (iii) NBS, PPh<sub>3</sub>, THF.

**Scheme 6.** Retrostructural Analysis of 2D Lam<sub>(k)</sub>, *p2mm* Simple Rectangular Columnar  $\Phi_{r,s}$ , *c2mm* Centered Rectangular Columnar ( $\Phi_{r,c}$ ), and Hexagonal Columnar ( $\Phi_h$ ) and of the 3D *la3d* Bicontinuous Cubic, 12-Fold Quasi-Liquid Crystal (QLC), *Pm3n* Cubic (Cub), *P4<sub>2</sub>/mnm* Tetragonal (Tet), and *Im3m* Cubic Lattices and Quasiperiodic Arrays



HBr in refluxing  $\text{CH}_3\text{COOH}$ , followed by re-esterification in acidic methanol (87–94% yield over two steps). **17a,b,d** were *O*-alkylated with 1-bromododecane in DMF using  $\text{K}_2\text{CO}_3$  (95–97% yield). Unlike benzyl or phenylpropyl analogues, the phenolates of the BpPr building blocks are not prone to oxidation and do not require thorough degassing. Reduction of **18a,b,d** with  $\text{LiAlH}_4$  in THF produced alcohols **19a,b,d** (85–98% yield), which could be converted to the corresponding bromides **20a,b,d** (94–99% yield) by treatment with  $\text{PPh}_3$  followed by NBS in THF.<sup>28</sup> *O*-Alkylation of **20a** onto **17b** or **17d** produced first generation dendrons (4BpPr-3,4BpPr)12G1- $\text{CO}_2\text{CH}_3$  (**22a**) and (4BpPr-3,4,5BpPr)12G1- $\text{CO}_2\text{CH}_3$  (**21a**), in 93% and 73% yield respectively. Repeated reduction and bromination provided the corresponding dendritic alcohols (**21b** and **22b**) in 86–87% yield and the dendritic bromides (**21c** and **22c**) in 75–92% yield.

**Synthesis of Higher-Generation Dendrons.** *O*-Alkylation of generation one dendritic bromides **20b**, **20d**, **21c**, and **22c** onto **17b**, **17c**, and **17d** (Scheme 5) provided three libraries of higher-generation constitutionally isomeric 3,4- and 3,5-disubstituted  $\text{AB}_2$  and 3,4,5-trisubstituted  $\text{AB}_3$  dendrons, respectively. Four new dendrons possessing  $-\text{CO}_2\text{CH}_3$  apex functionality were produced in each library at each generation. Reduction of the  $-\text{CO}_2\text{CH}_3$  apex group to  $-\text{CH}_2\text{OH}$  followed by bromination provided eight additional dendrons per generation per library. This iterative sequence of reactions was employed to synthesize dendrons up to the third generation. All dendrons in these generational libraries are composed of a generation one periphery group and a repeated interior 3,4-, 3,5-, or 3,4,5- branched building block. Each successive generation contains a further repetition of this interior building block.

**Structural and Retrostructural Analysis.** Structural and retrostructural analysis of the supramolecular dendrimers from the  $\text{AB}_3$  and the two  $\text{AB}_2$  libraries involved a variety of complementary techniques.  $^1\text{H}$  and  $^{13}\text{C}$  NMR, MALDI-TOF, and gel permeation chromatography (GPC) were employed to confirm the identity and purity of the dendrons. Differential scanning calorimetry (DSC), thermal optical polarized micro-

scopy (TOPM), experimental density ( $\rho_{20}$ ), and small- and wide-angle X-ray diffraction (XRD) experiments performed as a function of temperature on powder and oriented fibers, and computer modeling and XRD simulation allowed for phase identification and assignment, assessment of thermal transitions and corresponding enthalpies, and the determination of dimensions and features of the supramolecular objects self-organized into various lattices. Scheme 6 outlines the concept of structural and retrostructural analysis of the periodic lattices and quasiperiodic arrays formed from supramolecular dendrimers and dendronized polymers. All experimental details, analytical results, calculations, and simulation methodologies are available in the Supporting Information. The structural and retrostructural analysis was performed on supramolecular dendrimers self-assembled from dendrons containing  $-\text{CO}_2\text{CH}_3$  and  $-\text{CH}_2\text{OH}$  apex functionality.

Figures 2, 3, and 4 depict results obtained from small-angle X-ray scattering (SAXS), including the type of lattice formed, the diameter ( $D$ ) of the supramolecular sphere or supramolecular column, the projection of the solid angle ( $\alpha'$ )<sup>4b,18</sup> of the dendron, and the numbers of dendrons ( $\mu$ ) forming a supramolecular sphere or a 4.7 Å<sup>4b,c,18</sup> stratum of the supramolecular column. It is notable that all dendrons regardless of generation number or apex functionality self-assemble into supramolecular dendrimers that self-organize in various arrays (Tables 1–3, Supporting Information Figures SF1–SF13 and SF16–SF21, Supporting Information Tables ST1–ST3, ST5–ST7, and ST9–ST11). In the Supporting Information the retrostructural analysis of bilayer lamellar crystals (Lam<sub>(k,bilayer)</sub>) observed only at low temperature in the as-prepared state is reported. These structures are not included in Figures 2, 3, and 4. These structures are not reformed on subsequent cooling and reheating cycles, which makes discrimination between 1D, 2D, and 3D lattices difficult.

**Structural and Retrostructural Analysis of the  $\text{AB}_3$  Library of Supramolecular Dendrimers.** The first generation dendrons forming the periphery of all libraries including the  $\text{AB}_3$  library are (3,4,5BpPr)12G1-X, (3,4BpPr)12G1-X, (4BpPr-3,4,5BpPr)12G1-X, and (4BpPr-3,4BpPr)12G1-X. Subsequent generations consist

(28) Trippet, S. *J. Chem. Soc.* **1962**, 2337–2340.

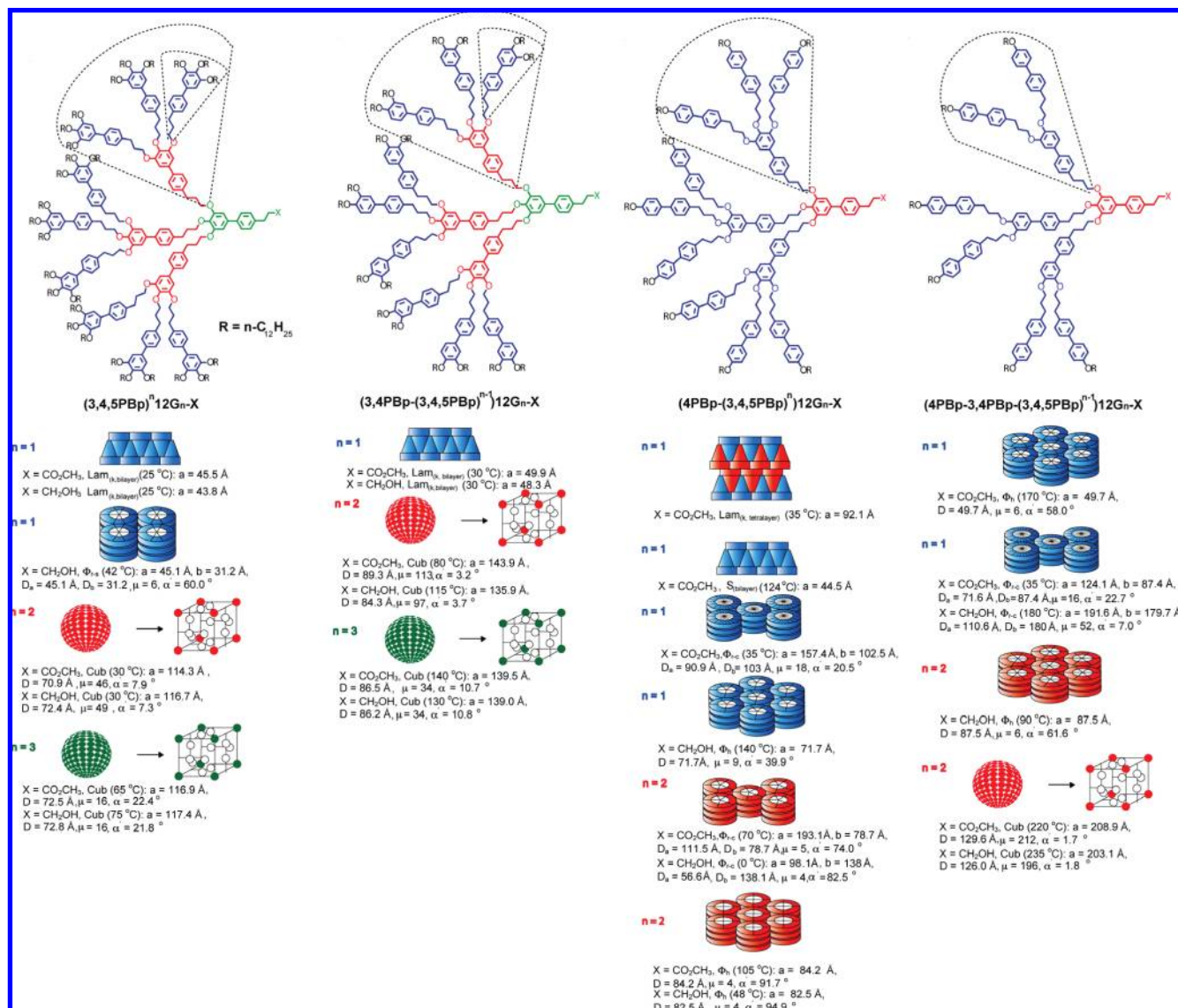


**Figure 2.** Structural and retrostructural analysis of supramolecular dendrimers self-assembled from AB<sub>3</sub> 3,4,5-trisubstituted dendrons.

of repetition of an identical branching unit, for example 3,4,5BpPr in the case of the AB<sub>3</sub> library. Libraries will be discussed from generation one upward. As demonstrated in previous studies,<sup>4b,c,18,29</sup> increasing the generation number results in a change of the molecular taper angle ( $\alpha$ ) and typically a transition from lamellar to columnar and to spherical self-assembly. Increasing generation number does not increase substantially the diameter of the supramolecular dendrimer ( $D$ ) but mostly reduces the number of dendrons ( $\mu$ ) required to form a supramolecular sphere or the cross section of a supramolecular column. Deviations from this pattern usually indicated hollow structures or novel mechanisms of self-assembly. For comparison updated figures containing the retrostructural analysis of benzyl ether (Supporting Figures SF23–25),<sup>4b</sup> phenyl propyl ether (Supporting Figures SF26–28),<sup>18</sup> and biphenyl 4-methyl ether supramolecular dendrimers (Supporting Figures SF29–30)<sup>19a</sup> have been provided in the Supporting Information.

For benzyl-<sup>4</sup> and biphenyl-4-methyl ether<sup>19a</sup> libraries, many generation one dendrons do not self-assemble. All phenylpropyl

ether dendrons self-assemble,<sup>18</sup> but many of their phase transitions occurred below room temperature. BpPr dendrons combine the advantage of pervasive self-assembly found for Pr dendrons with the higher phase transition temperatures provided by the Bp unit. Therefore, the first generation BpPr dendrons self-organize in Lam<sub>(k)</sub>, S,  $\Phi_{r-s}$ ,  $\Phi_{r-c}$ , and  $\Phi_{h,6}$  structures. The absence of spherical structures in generation one dendrons is in agreement with the generation one dendrons from the phenylpropyl ether library and is consistent with the few examples of benzyl ether and biphenyl-4-methyl ether dendrons that do self-assemble. Only the first generation dendrons (3,4,5BpPr)12G1-CO<sub>2</sub>CH<sub>3</sub> and (3,4BpPr)12G1-X do not exhibit a columnar phase forming exclusively Lam<sub>(k,bilayer)</sub> structures. Additionally, (4BpPr-3,4,5BpPr)12G1-CO<sub>2</sub>CH<sub>3</sub> exhibits a lamellar crystalline phase with a large layer spacing that cannot be explained by a bilayer structure. As will be discussed in a later section, a new tetralayer lamellar crystalline model (Lam<sub>(k,tetralayer)</sub>) was proposed.

Self-assembling dendrons that generate columnar assemblies are of interest for the design of electronic,<sup>13</sup> transport,<sup>14</sup> and mechanical<sup>16</sup> functions. Fortuitously, like their phenylpropyl ether counterparts, AB<sub>3</sub> BpPr, as well as 3,4-disubstituted AB<sub>2</sub>,

(29) Li, Y.; Lin, S.-T.; Goddard, W. A. *J. Am. Chem. Soc.* **2004**, *126*, 1872–1885.

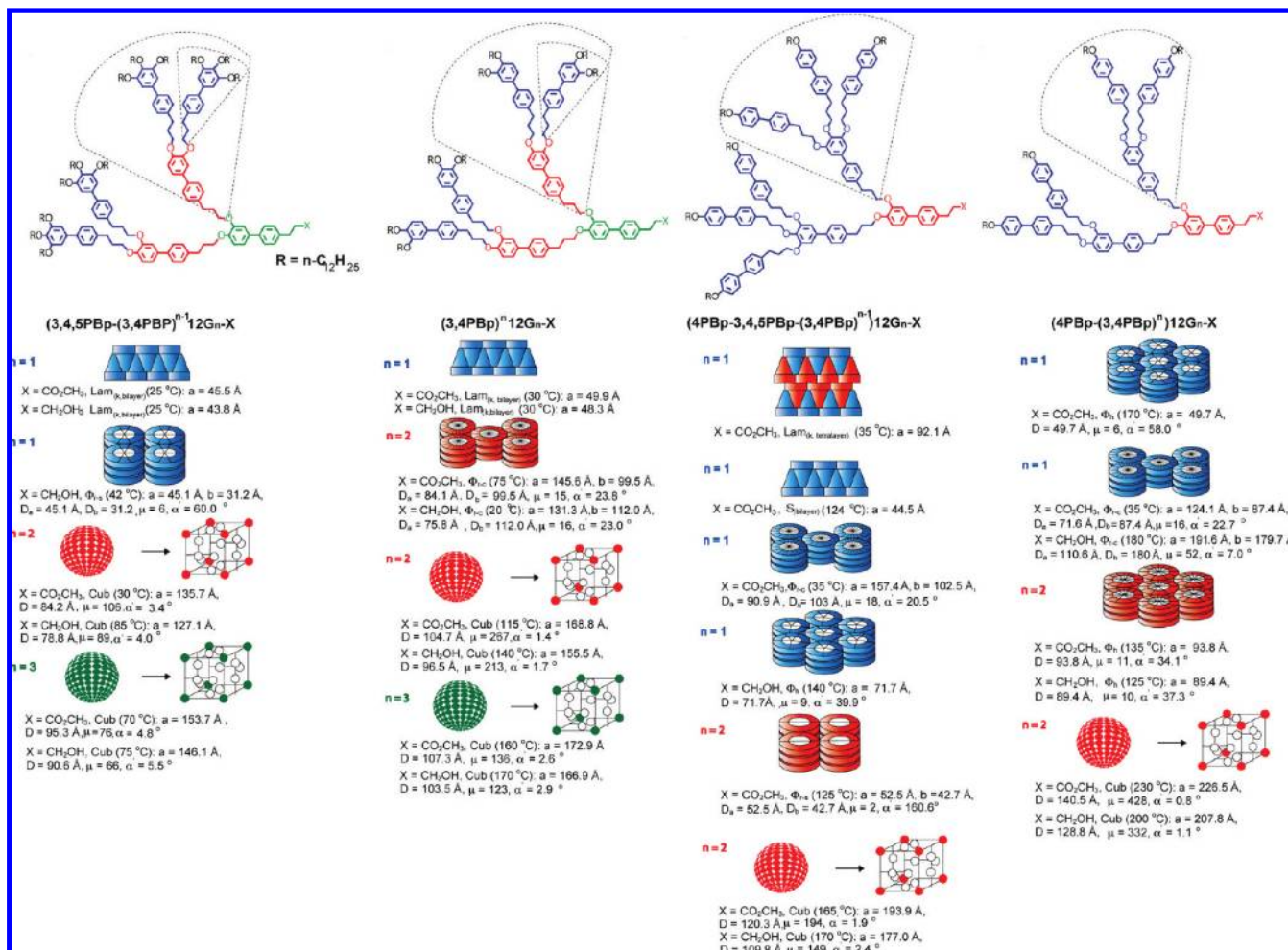


**Figure 3.** Structural and retrostructural analysis of supramolecular dendrimers self-assembled from  $AB_2$  3,4-disubstituted dendrons.

dendrons exhibit more columnar structures than the corresponding library of benzyl ether dendrons which almost exclusively form spherical supramolecular dendrimers self-organized in *Cub* lattices. Nevertheless, the  $AB_3$  library exhibits more spherical structures than the 3,5-disubstituted  $AB_2$  library.

As observed in previous libraries,  $(3,4,5BPpPr)^n12Gn-X$  and  $(3,4BPpPr-(3,4,5BPpPr)^{n-1})12Gn-X$  self-assemble into lamellar and columnar structures at generation one and into spherical structures self-organized in *Cub* lattices for generations two and three. The dimensions of the supramolecular spheres do not increase dramatically from generation two to three. In fact,  $(3,4,5BPpPr)^312G3-X$  self-organizes into supramolecular spheres that have a considerably smaller diameter than those of the spheres formed from any of the other BpPr dendrons of equivalent molecular dimensions. This result cannot be explained via self-assembly of dendrons in a conical conformation.<sup>4a</sup> In a later section, this finding will be explained by an alternative supramolecular spherical dendrimer assembled from spherically distorted short helical pyramidal columns as was previously demonstrated in the self-assembly of dendritic crowns.<sup>11,30</sup> It should be noted that the benzyl ether dendron  $(3,4-(3,4,5)^2)12G_3-CH_2OH$ <sup>8</sup> and phenylpropyl ether dendron  $(3,4,5Pr)^212G_2-CH_2OH$ <sup>18</sup> were found to form *QLC* arrays. The

absence of the *QLC* phase in the BpPr series may be indicative of slower self-assembly dynamics of the biphenyl-based building block. For biphenyl 4-methyl ether dendrons  $(3,4,5BPp)^212G_2-X$ , self-organization into  $\Phi_{r-s}$  and  $\Phi_h$  lattices was observed in addition to spherical supramolecular dendrimers. The absence of columnar phases for  $(3,4,5BPpPr)^212G_2-X$  could be due to the decrease in molecular taper angle induced by a longer dendritic building block.<sup>4b,18</sup> For  $(4BPp-(3,4,5BPpPr)^n)12Gn-X$ , only  $Lam_{(k)}$  and columnar structures in the first generation and exclusively columnar structures in the second generation were found. Upon increasing generation from  $(4BPp-3,4,5BPpPr)12G_1-CO_2CH_3$  to  $(4BPp-(3,4,5BPpPr)^2)12G_2-CO_2CH_3$ , there is a significant increase in the columnar diameter. For benzyl ether and phenylpropyl ether dendrons of similar primary structure, only columnar structures were observed at the first generation. At the second generation, columnar structures were found in both libraries, as well as a spherical *QLC* array for  $(4-(3,4,5)^2)12G_2-CO_2H$  and a *Cub* lattice for  $(4Pr-(3,4,5Pr)^2)12G_2-CH_2OH/COOH$ . It is not clear why  $(4BPp-(3,4,5BPpPr)^n)12Gn-X$  does not assemble in any spherical structures. For  $(4BPp-(3,4BPpPr)^n)12G_2-X$ , columnar structures are observed for generation one, and columnar and spherical structures are observed for generation two. This behavior is identical to phenylpropyl ether dendrons of similar primary structure, while analogous benzyl ether dendrons only form spherical *Cub* lattices for generation two and three. The  $\Phi_h$  lattice formed by  $(4BPp-3,4BPp-3,4,5BPpPr)12G_2-CH_2OH$  is significantly larger than those

(30) Percec, V.; Imam, M. R.; Peterca, M.; Wilson, D. A.; Graf, R.; Spiess, H. W.; Balagurusamy, V. S. K.; Heiney, P. A. *J. Am. Chem. Soc.* **2009**, *131*, 7662–7677.

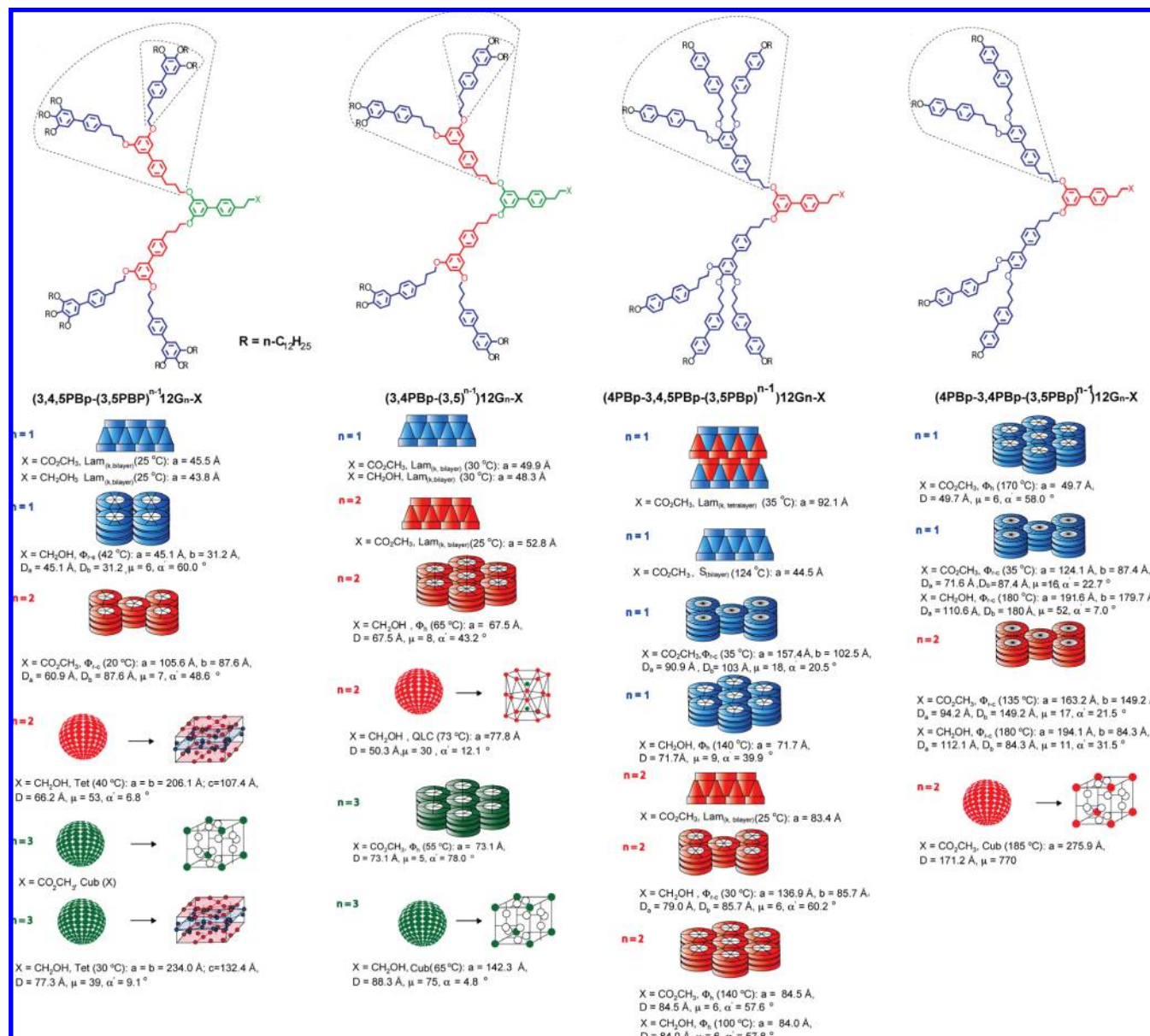


**Figure 4.** Structural and retrostructural analysis of supramolecular dendrimers self-assembled from AB<sub>2</sub> 3,5-disubstituted dendrons.

formed by (4BpPr-3,4BpPr)12G1-CO<sub>2</sub>CH<sub>3</sub>. As will be discussed in a later section, this deviation is explained in part by the fact that (4BpPr-3,4BpPr-3,4,5BpPr)12G2-CH<sub>2</sub>OH has a notable hollow center to the supramolecular column.

**Structural and Retrostructural Analysis of the 3,4-Disubstituted Library of AB<sub>2</sub> Supramolecular Dendrimers.** The design principles and the structures of the first generation dendrons in this library are equivalent to those in the AB<sub>3</sub> library. For comparison the retrostructural analysis of benzyl ether dendrons (Supporting Figure SF24),<sup>4b</sup> phenylpropyl ether dendrons (Supporting Figure SF27),<sup>18</sup> and biphenyl-4-methyl ether dendrons (Supporting Figures SF29–30)<sup>19a</sup> are provided. In previous libraries<sup>4b,18,19a</sup> and replicated with BpPr series of dendrons, the AB<sub>3</sub> and 3,4-disubstituted AB<sub>2</sub> libraries were found to be very similar. Not only does the 3,4-disubstituted AB<sub>2</sub> library of BpPr exhibit a similar ratio of spherical to columnar structures as the AB<sub>3</sub> library, but noncubic self-organization of spherical supramolecular dendrimers is also suppressed. As in the AB<sub>3</sub> library, BpPr dendrons exhibit slightly

more spherical structures than the corresponding biphenyl-4-methyl ether library, but less than the phenylpropyl and benzyl ether libraries.

Like all previously reported libraries, (3,4,5BpPr-(3,4BpPr)<sup>n-1</sup>)12Gn-X self-assembles exclusively into spherical supramolecular dendrimers at generation two and three, while Lam<sub>(k,bilayer)</sub> and Φ<sub>r-s</sub> structures are observed for generation one. All supramolecular spheres self-organize into Cub lattices, and the diameters of supramolecular spheres do not increase dramatically from generation two to three. For the phenylpropyl ether dendrons, (3,4,5Pr-3,4Pr)12G2-CH<sub>2</sub>OH and (3,4,5Pr-3,4Pr)12G2-CO<sub>2</sub>H self-organize into a QLC array and a Tet lattice, respectively. As for the AB<sub>3</sub> library, the absence of these phases may be evidence of slower self-assembly dynamics for BpPr dendrons. Like the phenylpropyl ether dendrons of similar primary structure, (3,4BpPr)<sup>n</sup>12Gn-X self-organizes into Lam<sub>(k,bilayer)</sub> phases at generation one, both Φ<sub>r-c</sub> and Cub lattices for generation two, and only Cub lattices at generation three.

**Table 1.** Thermal Transitions, Enthalpy Changes, and Phases Exhibited by the Library of 3,4,5-Trisubstituted Supramolecular Dendrimers

dendron	thermal transitions (°C) and corresponding enthalpy changes (kcal/mol) <sup>a</sup>		
	heating		cooling
(3,4,5BpPr)12G1-CO <sub>2</sub> CH <sub>3</sub>	Lam <sub>(k,bilayer)</sub> 12 (−6.19)	Lam <sub>(k,bilayer)</sub> 34 (22.25) i	i 6 (13.48) Lam <sub>(k,bilayer)</sub>
(3,4,5BpPr)12G1-CH <sub>2</sub> OH	Lam <sub>(k,bilayer)</sub> 12 (−6.38)	Lam <sub>(k,bilayer)</sub> 34 (22.48) i	i 23 (10.82) Φ <sub>r-s</sub> 18 (0.46) Φ <sub>r-s</sub> <sup>k</sup>
(3,4,5BpPr) <sup>2</sup> 12G2-CO <sub>2</sub> CH <sub>3</sub>	Lam <sub>(k,bilayer)</sub> 45 (15.31) i Φ <sub>r-s</sub> <sup>k</sup> 30 (1.55) Φ <sub>r-s</sub> 45 (15.34) i	Cub <sub>(k)</sub> 8 (2.47) Cub 35 (2.47) i Cub <sub>(k)</sub> 8 (2.28) Cub 35 (2.65) i	i 32 (3.00) Cub −8 (3.32) Cub <sub>(k)</sub>
(3,4,5BpPr) <sup>2</sup> 12G2-CH <sub>2</sub> OH	Cub <sub>(k)</sub> −6 Cub 77 (2.02) i Cub <sub>(k)</sub> −6 Cub 76 (3.12) i		i 73 (2.29) Cub −19 (1.72) Cub <sub>(k)</sub>
(3,4,5BpPr) <sup>2</sup> 12G3-CO <sub>2</sub> CH <sub>3</sub>	Cub <sub>(k)</sub> −10 (11.89) Cub 83 (0.40) i Cub <sub>(k)</sub> −11 (11.21) Cub 76 (0.48) i		i 73 (2.29) Cub −18 (10.05) Cub <sub>(k)</sub>
(3,4,5BpPr) <sup>2</sup> 12G3-CH <sub>2</sub> OH	Cub <sub>(k)</sub> −11 (16.59) Cub 94 (1.01) i Cub <sub>(k)</sub> −11 (17.89) Cub 94 (0.0) i		i −18 (17.89) Cub 97 (0.8)
(3,4BpPr-3,4,5BpPr)12G2-CO <sub>2</sub> CH <sub>3</sub>	Cub <sub>(k)</sub> 60 (16.52) 61(1.77) Cub 101 (7.51) i Cub <sub>(k)</sub> 39 (−6.72) 58 (6.06) Cub 101 (7.53) i		i 100 (8.30) Cub 16 (4.22) Cub <sub>(k)</sub>
(3,4BpPr-3,4,5BpPr)12G2-CH <sub>2</sub> OH	Cub <sub>(k)</sub> 67 (15.29) Cub 129 (7.18) i Cub <sub>(g)</sub> 65 (0.66) Cub 129 (7.18) i		i 128 (7.52) Cub 60 Cub <sub>(g)</sub>
(3,4BpPr-(3,4,5BpPr) <sup>2</sup> )12G3-CO <sub>2</sub> CH <sub>3</sub>	Cub <sub>(k)</sub> 63 (17.26) Cub 156 (12.05) i Cub <sub>(g)</sub> 63 Cub 156 (12.59) i		i 154 (8.33) Cub 63 Cub <sub>(g)</sub>
(3,4BpPr-(3,4,5BpPr) <sup>2</sup> )12G3-CH <sub>2</sub> OH	Cub <sub>(k)</sub> 67 (48.89) Cub 169 (16.14) i Cub <sub>(g)</sub> 66 Cub 169 (15.86) i		i 168 (16.70) Cub 66 Cub <sub>(g)</sub>
(4BpPr-3,4,5BpPr)12G1-CO <sub>2</sub> CH <sub>3</sub>	Φ <sub>r-c</sub> 90 (1.83) Lam <sub>(k,tetralayer)</sub> 132 (20.73) i Lam <sub>(k,tetralayer)</sub> 132 (20.26) i		i 125 (4.04) S <sub>(bilayer)</sub> 114 (15.49) Lam <sub>(k,tetralayer)</sub>
(4BpPr-3,4,5BpPr)12G1-CH <sub>2</sub> OH	Lam <sub>(k,bilayer)</sub> 94 (4.81) Φ <sub>h</sub> <sup>io</sup> 111 (9.56) Φ <sub>h</sub> 146 (6.74) i Φ <sub>h</sub> <sup>io</sup> 112 (10.02) Φ <sub>h</sub> 146 (6.78) i		i 145 (6.71) Φ <sub>h</sub> 92 (9.86) Φ <sub>h</sub>
(4BpPr-(3,4,5BpPr) <sup>2</sup> )12G2-CO <sub>2</sub> CH <sub>3</sub>	Φ <sub>r-c</sub> <sup>k</sup> 55 (49.78) Φ <sub>r-c</sub> 82 (15.46) Φ <sub>h</sub> 131 (0.73) i Φ <sub>r-c</sub> 30 (−32.05) Φ <sub>r-c</sub> <sup>k</sup> 55 (36.54) Φ <sub>r-c</sub> 83 (14.91) Φ <sub>h</sub> 130 (0.04) i		i 122 (0.06) Φ <sub>h</sub> 70 (23.38) Φ <sub>r-c</sub>
(4BpPr-(3,4,5BpPr) <sup>2</sup> )12G2-CH <sub>2</sub> OH	Φ <sub>r-c</sub> <sup>k</sup> 89 (29.8) Φ <sub>h</sub> 125 (0.1) i Φ <sub>r-c</sub> 81 (14.8) Φ <sub>h</sub> 125 (0.1) i		i 124 (0.1) Φ <sub>h</sub> 81 (14.8) Φ <sub>r-c</sub>
(4BpPr-3,4BpPr-3,4,5BpPr)12G2-CO <sub>2</sub> CH <sub>3</sub>	Cub <sub>(k)</sub> 77 (21.75) Cub 243 (16.94) i Cub <sub>(k)</sub> 71 (6.76) Cub <sub>(g)</sub> Cub 244 (13.83) i		i 240 (20.34) Cub Cub <sub>(g)</sub> 57 (6.32) Cub <sub>(k)</sub>
(4BpPr-3,4BpPr-3,4,5BpPr)12G2-CH <sub>2</sub> OH	Φ <sub>h</sub> <sup>io</sup> 61 (2.89) Φ <sub>h</sub> 180 Cub 248 (16.59) i Φ <sub>h</sub> <sup>io</sup> 70 (0.80) Φ <sub>h</sub> 180 Cub 248 (9.24) i		i 238 (7.73) Cub 180 Φ <sub>h</sub> 50 (1.21) Φ <sub>h</sub> <sup>io</sup>

<sup>a</sup> Thermal transitions (°C) and enthalpy changes (kcal/mol) were determined by DSC (10 °C/min), data from the first heating and cooling scans are on the first line, and the data from the second heating are on the second line; S<sub>(bilayer)</sub> = smectic bilayer lattice; Lam<sub>(k,bilayer)</sub> = lamellar crystal with two layer repeat; Lam<sub>(k,tetralayer)</sub> = banana-like lamellar crystal with four layer repeat; Φ<sub>r-c</sub> = *c2mm* centered rectangular columnar lattice; Φ<sub>r-c</sub><sup>k</sup> = crystalline *c2mm* centered rectangular columnar lattice; Φ<sub>h</sub> = *p6mm* hexagonal columnar lattice; Φ<sub>h</sub><sup>io</sup> = hexagonal columnar lattice with internal order; Cub = *Pm3n* cubic lattice; Cub<sub>(k)</sub> = crystalline *Pm3n* cubic lattice; Cub<sub>(g)</sub> = glassy *Pm3n* cubic lattice; i = isotropic.

For analogous benzyl ether and biphenyl-4-methyl ether dendrons, only *Cub* lattices were observed for generation two and three. (4BpPr-3,4,5BpPr)12G1-X self-organizes into Lam<sub>(k,bilayer)</sub> and columnar structures, while (4BpPr-3,4,5BpPr-3,4BpPr)12G2-X exhibits columnar and *Cub* structures. The corresponding generation two benzyl- and phenylpropyl ether dendrons only form spherical structures. The persistence of columnar structures in the present case is not readily explained but is welcomed considering their synthetic utility. (4BpPr-(3,4BpPr)<sup>2</sup>)12G2-X self-organizes into both columnar and spherical structures. This is identical to what was observed for phenylpropyl ether dendrons; while similar benzyl ether dendrons exclusively self-organized into *Cub* lattices, biphenyl-methyl ether dendrons self-organized only into Φ<sub>r-s</sub> assemblies. The Φ<sub>h</sub> and *Cub* phase generated by (4BpPr-(3,4BpPr)<sup>2</sup>)12G2-X are larger than the expected 90–100 Å diameters, and in later sections this is explained through hollow columnar and hollow spherical models. For (4BpPr-(3,4BpPr)<sup>2</sup>)12G2-CO<sub>2</sub>CH<sub>3</sub> an experimental spherical diameter of ~140 Å was observed. The corresponding dendritic alcohol (4BpPr-(3,4BpPr)<sup>2</sup>)12G2-CH<sub>2</sub>OH self-assembles into smaller supramolecular spheres, ~128 Å in diameter, due to H-bonding interactions between neighboring apex groups which destabilize and diminish the hollow center. That (4BpPr-(3,4BpPr)<sup>2</sup>)12G2-CO<sub>2</sub>CH<sub>3</sub> forms both hollow columns and hollow spheres suggests similar design principles for both supramolecular architectures.

**Structural and Retrostructural Analysis of the 3,5-Disubstituted Library of AB<sub>2</sub> Supramolecular Dendrimers.** The design principles and the structures of the first generation dendrons in this library are equivalent to those in the AB<sub>3</sub> library. For

comparison the retrostructural analysis of benzyl ether dendrons (Supporting Figure SF25),<sup>4b</sup> phenylpropyl ether dendrons (Supporting Figure SF28),<sup>18</sup> and biphenyl-4-methyl ether dendrons (Supporting Figures SF29–30)<sup>19a</sup> are provided. The most striking feature of the 3,5-disubstituted library of AB<sub>2</sub> BpPr dendrons is that it contains the greatest diversity of self-organized lattices and the smallest number of supramolecular spheres. Examples of Lam<sub>(k)</sub>, S, Φ<sub>h</sub>, Φ<sub>r-s</sub>, Φ<sub>r-c</sub>, *Cub*, *Tet*, and *QLC* lattices and arrays are present. This is the constitutionally isomeric library of the corresponding 3,4-disubstituted AB<sub>2</sub> library of dendrons. Therefore, this library is expected to self-assemble in different supramolecular structures than its 3,4-constitutionally isomeric library. When similar structures are observed, their mechanisms of self-assembly must be different. In AB<sub>3</sub> and 3,4-disubstituted AB<sub>2</sub> libraries a higher than expected number of columnar structures were observed. Consistent with the constitutional isomerism of the 3,5-disubstituted library of AB<sub>2</sub> BpPr dendrons, this trend is reversed and more spherical structures are present than in any previous 3,5-disubstituted library.<sup>4b,18,19a</sup>

(3,4,5BpPr-(3,5BpPr)<sup>n-1</sup>)12Gn-X forms Lam<sub>(k,bilayer)</sub> and Φ<sub>r-s</sub> structures at generation one, Φ<sub>r-c</sub> for the generation two ester, and a *Tet* lattice composed of spherical supramolecular dendrimers for the generation two alcohol. At generation three only spherical supramolecular dendrimers that self-organize into an unknown cubic lattice for the ester and a *Tet* lattice for the alcohol were observed. For the phenylpropyl ether dendrons (3,4,5Pr-(3,5Pr)<sup>n-1</sup>)12Gn-X, the transitions from columnar to *Tet* lattices did not occur until generation three. A *QLC* array was observed for (3,4,5-(3,5)<sup>2</sup>)12G3-CH<sub>2</sub>OH but is not present for

**Table 2.** Thermal Transitions, Enthalpy Changes, and Phases Exhibited by the Library of 3,4-Disubstituted Supramolecular Dendrimers

dendron	thermal transitions (°C) and corresponding enthalpy changes (kcal/mol) <sup>a</sup>	
	heating	cooling
(3,4,5BpPr-3,4BpPr)12G2-CO <sub>2</sub> CH <sub>3</sub>	Cub <sub>(k)</sub> 11 (3.69) Cub 58 (5.61) i Cub 58 (5.72) i	i 56 (5.78) Cub
(3,4,5BpPr-3,4BpPr)12G2-CH <sub>2</sub> OH	Cub <sub>(k)</sub> 10 (1.26) Cub 92 (3.87) i Cub 92 (3.71) i	i 91 (3.88) Cub
(3,4,5BpPr-(3,4BpPr) <sup>2</sup> )12G3-CO <sub>2</sub> CH <sub>3</sub>	Cub 121 (5.52) i Cub 121 (5.91) i	i 117 (6.40) Cub
(3,4,5BpPr-(3,4BpPr) <sup>2</sup> )12G3-CH <sub>2</sub> OH	Cub 133 (2.88) i Cub 133 (2.63) i	i 129 (2.90) Cub
(3,4BpPr)12G1-CO <sub>2</sub> CH <sub>3</sub>	Lam <sub>(k,bilayer)</sub> 75 (16.74) i Lam <sub>(k,bilayer)</sub> 74 (16.90) i	i 62 (15.88) Lam <sub>(k,bilayer)</sub>
(3,4BpPr)12G1-CH <sub>2</sub> OH	Lam <sub>(k,bilayer)</sub> 86 (18.47) i Lam <sub>(k,bilayer)</sub> 86 (18.61) i	i 78 (18.46) Lam <sub>(k,bilayer)</sub>
(3,4BpPr) <sup>2</sup> 12G2-CO <sub>2</sub> CH <sub>3</sub>	Φ <sub>r-c</sub> <sup>k</sup> 50 (2.86) Φ <sub>r-c</sub> 85 (10.01) Cub 123 (7.50) i Φ <sub>r-c</sub> <sup>k</sup> 46 (0.31) Φ <sub>r-c</sub> 83 (4.12) Cub 121 (7.57) i	i 121 (7.57) Cub 32 (4.62) Φ <sub>r-c</sub> <sup>k</sup>
(3,4BpPr) <sup>2</sup> 12G2-CH <sub>2</sub> OH	Lam <sub>(k,bilayer)</sub> 47 (6.04) Φ <sub>r-c</sub> <sup>io</sup> 74 (2.63) Cub 149 (18.13) i Φ <sub>r-c</sub> <sup>io</sup> 41 (3.80) Cub 149 (17.84) i	i 147 (18.43) Cub 29 (4.73) Φ <sub>r-c</sub> <sup>io</sup>
(3,4BpPr) <sup>3</sup> 12G3-CO <sub>2</sub> CH <sub>3</sub>	Cub 185 (14.36) i Cub 185 (14.22) i	i 184 (14.25) Cub
(3,4BpPr) <sup>3</sup> 12G3-CH <sub>2</sub> OH	Cub 196 (12.74) i Cub 196 (13.17) i	i 195 (13.81) Cub
(4BpPr-3,4,5BpPr-3,4BpPr)12G2-CO <sub>2</sub> CH <sub>3</sub>	Lam <sub>(k,bilayer)</sub> 136 (12.22) Φ <sub>r-s</sub> <sup>k</sup> 145 (5.11) Cub 172 (12.56) i Cub <sub>(k)</sub> 100 (-10.65) Φ <sub>r-s</sub> <sup>k</sup> 136 (14.58) Cub 172 (12.49) i	i 171 (12.67) Cub 87 (13.02) Cub <sub>(k)</sub>
(4BpPr-3,4,5BpPr-3,4BpPr)12G2-CH <sub>2</sub> OH	Lam <sub>(k,bilayer)</sub> 106 (15.05) Φ <sub>x</sub> 127 (7.79) Cub 188 (13.25) i Φ <sub>x</sub> + Cub <sub>(k)</sub> 128 (5.51) Cub 188 (13.91) i	i 186 (14.15) Cub 95 (11.11) Φ <sub>x</sub> + Cub <sub>(k)</sub>
(4BpPr-3,4BpPr)12G1-CO <sub>2</sub> CH <sub>3</sub>	Lam <sub>(k,bilayer)</sub> 69 (0.71) 91 (-3.50) Φ <sub>r-c</sub> <sup>k1</sup> 112 (10.15) Φ <sub>h</sub> 179 (4.14) i Φ <sub>r-c</sub> <sup>k2</sup> 69 (0.68) 91 (-3.79) Φ <sub>r-c</sub> <sup>k1</sup> 110 (10.23) Φ <sub>h</sub> 179 (4.50) i	i 177 (4.95) Φ <sub>h</sub> 84 (7.79) Φ <sub>r-c</sub> <sup>k2</sup>
(4BpPr-3,4BpPr)12G1-CH <sub>2</sub> OH	Lam <sub>(k,bilayer)</sub> 115 (14.21) Φ <sub>r-c</sub> 187 (8.14) i Φ <sub>r-c</sub> <sup>io</sup> 111 (7.38) Φ <sub>r-c</sub> 187 (8.09) i	i 185 (8.71) Φ <sub>r-c</sub> 96 (8.79) Φ <sub>r-c</sub> <sup>io</sup>
(4BpPr-(3,4BpPr) <sup>2</sup> )12G2-CO <sub>2</sub> CH <sub>3</sub>	Lam <sub>(k,bilayer)</sub> 94 (3.25) Φ <sub>h</sub> <sup>io</sup> 137 (0.09) Cub 242 (2.50) i Cub <sub>(k)</sub> 70 (1.31) Cub 242 (2.45) i	i 241 (2.66) Cub 57 (1.19) Cub <sub>(k)</sub>
(4BpPr-(3,4BpPr) <sup>2</sup> )12G2-CH <sub>2</sub> OH	Lam <sub>(k,bilayer)</sub> 57 (0.58) Φ <sub>h</sub> <sup>io</sup> 103 (0.02) Cub 255 (1.65) i Cub <sub>(k)</sub> 67 (0.38) Cub 255 (1.64) i	i 248 (1.81) Cub 55 (0.32) Cub <sub>(k)</sub>

<sup>a</sup> Thermal transitions (°C) and enthalpy changes (kcal/mol) were determined by DSC (10 °C/min), data from the first heating and cooling scans are on the first line, and the data from the second heating are on the second line; Lam<sub>(k,bilayer)</sub> = lamellar crystal with two layer repeat; Φ<sub>x</sub> = unknown columnar lattice; Φ<sub>r-c</sub> = *c2mm* centered rectangular columnar lattice; Φ<sub>r-c</sub><sup>k</sup> = crystal *c2mm* centered rectangular columnar lattice; Φ<sub>r-c</sub><sup>io</sup> = rectangular columnar lattice with internal order; Φ<sub>r-s</sub><sup>k</sup> = crystal *p2mm* simple rectangular columnar lattice; Φ<sub>h</sub> = *p6mm* hexagonal columnar lattice; Φ<sub>h</sub><sup>io</sup> = hexagonal columnar lattice with internal order; Cub<sub>(k)</sub> = crystal *Pm3n* cubic lattice; Cub = *Pm3n* cubic lattice; i = isotropic.

**Table 3.** Thermal Transitions, Enthalpy Changes, and Phases Exhibited by the Library of 3,5-Disubstituted Supramolecular Dendrimers

dendron	Thermal transitions (°C) and the corresponding enthalpy changes (kcal/mol) <sup>a</sup>	
	heating	cooling
(3,4,5BpPr-3,5BpPr)12G2-CO <sub>2</sub> CH <sub>3</sub>	Φ <sub>r-c</sub> <sup>k</sup> 9 (8.57) Φ <sub>r-c</sub> 25 (4.43) i Φ <sub>r-c</sub> <sup>k</sup> 9 (8.46) Φ <sub>r-c</sub> 23 (2.66) i	i -1 (7.49) Φ <sub>r-c</sub> <sup>k</sup>
(3,4,5BpPr-3,5BpPr)12G2-CH <sub>2</sub> OH	Tet 44 (1.32) i Tet 43 (1.46) i	i 40 (1.22) Tet
(3,4,5BpPr-(3,5BpPr) <sup>2</sup> )12G3-CO <sub>2</sub> CH <sub>3</sub>	Cub <sub>(x)</sub> -3 (6.96) i Cub <sub>(x)</sub> -2 (6.83) i	i -17 (6.11) Cub <sub>(x)</sub>
(3,4,5BpPr-(3,5BpPr) <sup>2</sup> )12G3-CH <sub>2</sub> OH	Tet <sub>(k)</sub> -2 (3.64) Tet 38 (0.17) i Tet <sub>(k)</sub> -2 (4.62) Tet 38 (0.18) i	i 36 (0.23) Tet -17 (2.64) Tet <sub>(k)</sub>
(3,4BpPr-3,5BpPr)12G2-CO <sub>2</sub> CH <sub>3</sub>	Lam <sub>(k,bilayer)</sub> 91 (11.11) Lam <sub>(k,bilayer)</sub> 95 (24.58) i Lam <sub>(k,bilayer)</sub> 15 (2.14) Lam <sub>(k,bilayer)</sub> 52 (-7.01) Lam <sub>(k,bilayer)</sub> 92 (33.1) i	i 48 (30.3) Lam <sub>(k,bilayer)</sub>
(3,4BpPr-3,5BpPr)12G2-CH <sub>2</sub> OH	Lam <sub>(k,bilayer)</sub> 55 (9.49) Φ <sub>h</sub> 74 (3.41) i Φ <sub>h</sub> <sup>io</sup> 50 (5.45) Φ <sub>h</sub> 74 (3.44) i	i 73 (3.61) Φ <sub>h</sub> 33 (4.86) Φ <sub>h</sub> <sup>io</sup>
(3,4BpPr-(3,5BpPr) <sup>2</sup> )12G3-CO <sub>2</sub> CH <sub>3</sub>	Φ <sub>h</sub> <sup>io</sup> 57 (27.75) i Φ <sub>h</sub> <sup>io</sup> 57 (8.83) i	i 55 (6.97) Φ <sub>h</sub> <sup>io</sup>
(3,4BpPr-(3,5BpPr) <sup>2</sup> )12G3-CH <sub>2</sub> OH	Lam <sub>(k,bilayer)</sub> 62 (38.83) Cub 77 (7.63) i Cub 77 (8.10) i	i 75 (7.68) Cub
(4BpPr-3,4,5BpPr-3,5BpPr)12G2-CO <sub>2</sub> CH <sub>3</sub>	Lam <sub>(k,bilayer)</sub> 98 (25.98) Φ <sub>h</sub> 152 (11.18) i Lam <sub>(k,bilayer)</sub> 94 (17.43) Φ <sub>h</sub> 152 (11.27) i	i 150 (11.21) Φ <sub>h</sub> 88 (18.56) Lam <sub>(k,bilayer)</sub>
(4BpPr-3,4,5BpPr-3,5BpPr)12G2-CH <sub>2</sub> OH	Lam <sub>(k,bilayer)</sub> 96 (29.11) Φ <sub>h</sub> 162 (13.01) i Φ <sub>r-c</sub> <sup>io</sup> 87 (9.88) Φ <sub>h</sub> 162 (13.66) i	i 161 (13.55) Φ <sub>h</sub> 87 (9.88) Φ <sub>r-c</sub> <sup>io</sup>
(4BpPr-3,4BpPr-3,5BpPr)12G2-CO <sub>2</sub> CH <sub>3</sub>	Lam <sub>(k,bilayer)</sub> 94 (2.47) Φ <sub>r-c</sub> <sup>io</sup> 140 (14.56) Cub 195 (10.57) i Φ <sub>r-c</sub> <sup>io</sup> 96 (-11.06) Φ <sub>r-c</sub> <sup>io</sup> 141 (13.19) Cub 195 (9.71) i	i 194 (13.18) Cub 63 (8.89) Φ <sub>r-c</sub> <sup>io</sup>
(4BpPr-3,4BpPr-3,5BpPr)12G2-CH <sub>2</sub> OH	Lam <sub>(k,bilayer)</sub> 94 (21.53) Φ <sub>r-c</sub> 201 (12.83) i Φ <sub>r-c</sub> <sup>io</sup> 88 (3.71) Φ <sub>r-c</sub> 203 (14.22) i	i 203 (14.14) Φ <sub>r-c</sub> 88 (3.71) Φ <sub>r-c</sub> <sup>io</sup>

<sup>a</sup> Thermal transitions (°C) and enthalpy changes (kcal/mol) were determined by DSC (10 °C/min), data from the first heating and cooling scans are on the first line, and the data from the second heating are on the second line; Lam<sub>(k,bilayer)</sub> = lamellar crystal with two layer repeat; Φ<sub>r-s</sub> = *p2mm* simple rectangular columnar lattice; Φ<sub>r-c</sub> = *c2mm* centered rectangular columnar lattice; Φ<sub>r-c</sub><sup>k</sup> = crystal *c2mm* centered rectangular columnar lattice; Φ<sub>h</sub> = *p6mm* hexagonal columnar lattice; Φ<sub>h</sub><sup>io</sup> = hexagonal columnar lattice with internal order; Tet = *P4<sub>2</sub>/mnm* tetragonal lattice; Tet<sub>(k)</sub> = crystal *P4<sub>2</sub>/mnm* tetragonal lattice; Cub = *Pm3n* cubic lattice; X = unknown lattice; i = isotropic.

(3,4,5BpPr-(3,5BpPr)<sup>2</sup>)12G3-X. For (3,4BpPr-(3,5BpPr)<sup>n</sup>)12Gn-X, only Lam<sub>(k,bilayer)</sub> structures were found for generation one and the generation two ester, though Φ<sub>h</sub> and a monotropic QLC

phase upon slow cooling (Supporting Information Figure SF13) were observed for the generation two alcohol. For (3,4BpPr-(3,5BpPr)<sup>2</sup>)12G2-X, a Φ<sub>h</sub> lattice is observed for the ester and

the corresponding alcohol self-organizes into a *Cub* lattice. The columnar and spherical structures do not differ dramatically in dimensions from generation two to three. This behavior is similar to that of the corresponding biphenyl-4-methyl ether dendrons, wherein  $\Phi_h$  structures were observed for the generation two and three esters and a *Cub* lattice was found for the generation two alcohol. Benzyl and phenylpropyl ether dendrons of similar primary structure self-organize exclusively into columnar lattices. The appearance of spherical self-assembly at generation two and three for (3,4BpPr-(3,5BpPr)<sup>n</sup>)12Gn-X may be due in part to the increased length of the BpPr building block which decreases the molecular taper angle. Like all previously reported libraries (4BpPr-3,4,5BpPr-3,4BpPr)12Gn-X and its generation one precursor (4BpPr-3,4,5BpPr)12G1-X form only lamellar and columnar structures.

In previous libraries, new self-assembly mechanisms were discovered via unexpected differences in supramolecular size and shape with increased generation number. Increased supramolecular diameter at higher generation has been used to identify self-assembly into structures with a hollow center,<sup>12</sup> while a reversal in the order of the columnar and spherical self-assembly indicated new mechanisms of column formation such as dendron backfolding.<sup>17</sup> Here, the discovery of a new mechanism of self-assembly was signaled by unexpected similarities between constitutionally isomeric dendrons. (4BpPr-(3,4BpPr)<sup>2</sup>)12G2-CO<sub>2</sub>CH<sub>3</sub> and (4BpPr-3,4BpPr-3,5BpPr)12G2-CO<sub>2</sub>CH<sub>3</sub> both are large supramolecular spherical dendrimers that self-organize into a *Cub* lattice. In the benzyl and phenylpropyl ether libraries the primary structure (4-3,4-3,5) results in only columnar structures and has been used extensively in the construction of functional porous columnar materials.<sup>14</sup> As expected (4BpPr-3,4BpPr-3,5BpPr)12G2-X forms a columnar structure at room temperature. However, at higher temperature (4BpPr-3,4BpPr-3,5BpPr)12G2-CO<sub>2</sub>CH<sub>3</sub> transforms from a  $\Phi_{r-c}$  to a *Cub* lattice like its constitutional isomer (4BpPr-(3,4BpPr)<sup>2</sup>)12G2-CO<sub>2</sub>CH<sub>3</sub>. This anomalous finding, which was also noted in the corresponding biphenyl-4-methyl ether library, led to the discovery of the most significant new phase elucidated through the synthesis of BpPr dendrons. (4BpPr-3,4BpPr-3,5BpPr)12G2-CO<sub>2</sub>CH<sub>3</sub> self-assembles into spherical supramolecular dendrimers with experimental diameters of 171.2 Å. As will be discussed in a later section, the experimental spherical diameter is far too large to be explained by a hollow central cavity and suggests a novel interdigitated vesicular form of spherical self-assembly.

**Banana-like Lamellar Crystal with Four-Layer Repeat.** Many generation one BpPr dendrons form lamellar phases. In most cases, such as in the case of (3,4BpPr)12G1-CO<sub>2</sub>CH<sub>3</sub>, the *d*-spacings were consistent with the dimensions of a dendron bilayer assuming ~30% compression<sup>31</sup> of aliphatic domains, interdigitation, or tilt to the dendron. (3,4,5BpPr)12G1-CH<sub>2</sub>OH has molecular dimensions similar to those of (3,4BpPr)12G1-CO<sub>2</sub>CH<sub>3</sub>, but XRD showed smaller *d*-spacings. This can be explained by a greater degree of interdigitation of the aryl segment.

Anomalously, (4BpPr-3,4,5BpPr)12G1-CO<sub>2</sub>CH<sub>3</sub> exhibits a *d*-spacing of 92.1 Å (see Supporting Figure SF21) that is significantly larger than expected for a molecular dimer even if the aliphatic tails were in an unrealistically extended all-*trans* conformation (86 Å). Additionally, wide-angle XRD shows

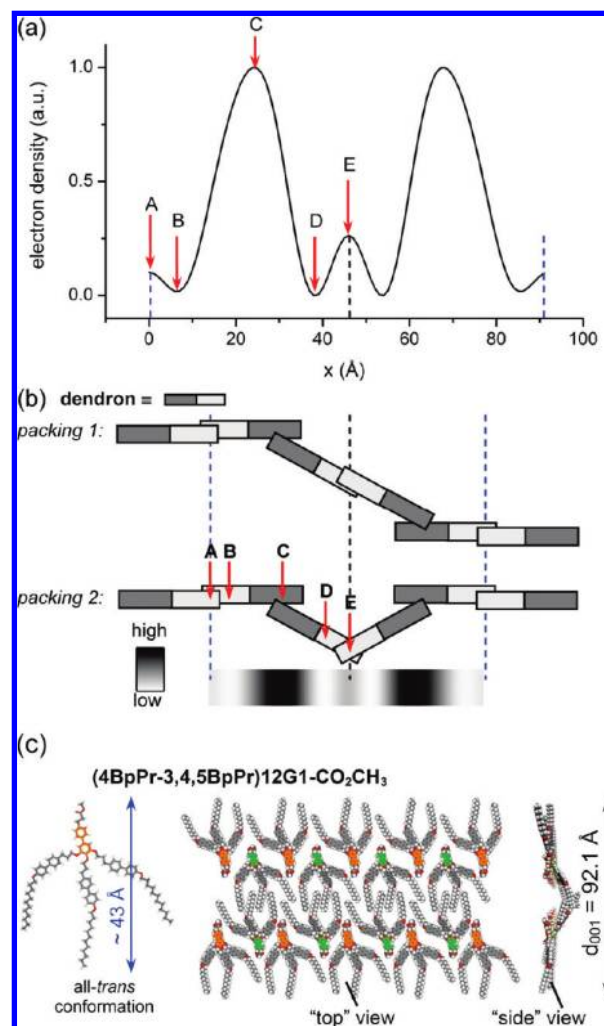


**Figure 5.** Lamellar crystalline structure with four layer repeat observed for (4BpPr-3,4,5BpPr)12G1-CO<sub>2</sub>CH<sub>3</sub>. (a) Electron density map indicating decreased electron density in every other layer. (b) Proposed packing models together with the electron density map. (c) Molecular model of (4BpPr-3,4,5BpPr)12G1-CO<sub>2</sub>CH<sub>3</sub> and the top and side view of the puckered tetralayer model.

sharp reflections indicative of a crystalline structure, in contrast to broader wide-angle reflections for the monotropic *S*<sub>(bilayer)</sub> structure formed upon slow cooling from the isotropic phase (Supporting Figure SF22). A reconstructed electron density map of the lamellar crystalline structure (Figure 5a) suggests increased crystallinity, accompanied by a decrease in electron density in every other layer. The increase in crystallinity likely induces chain tilting to compensate in the reduction of the alkyl tail cross-sectional area. A four layer model for this lamellar crystalline phase was proposed where the internal layers are either tilted or puckered (Figure 5b, packing 1 and 2). A molecular model of the puckered conformation is depicted in Figure 5c. The shape of this lamellar crystal resembles a supramolecular equivalent of ferroelectric or antiferroelectric lamellar structures formed from polar banana-shaped molecules.<sup>32</sup>

**Dimensions and Mechanism of Self-Assembly into Spherical Supramolecular Dendrimers Is Determined through Branching Pattern.** Self-organization of dendrons into the *Pm* $\bar{3}$ *n* cubic phase was first observed for (3,4,5)<sup>n</sup>12Gn-X, and a model of self-

(31) Percec, V.; Peterca, M.; Tsuda, Y.; Rosen, B. M.; Uchida, S.; Imam, M. R.; Ungar, G.; Heiney, P. A. *Chem.—Eur. J.* **2009**, *15*, 8994–9004.

(32) Takazoe, H.; Takanishi, Y. *Jpn. J. Appl. Phys., Part 1* **2006**, *45*, 597–625.

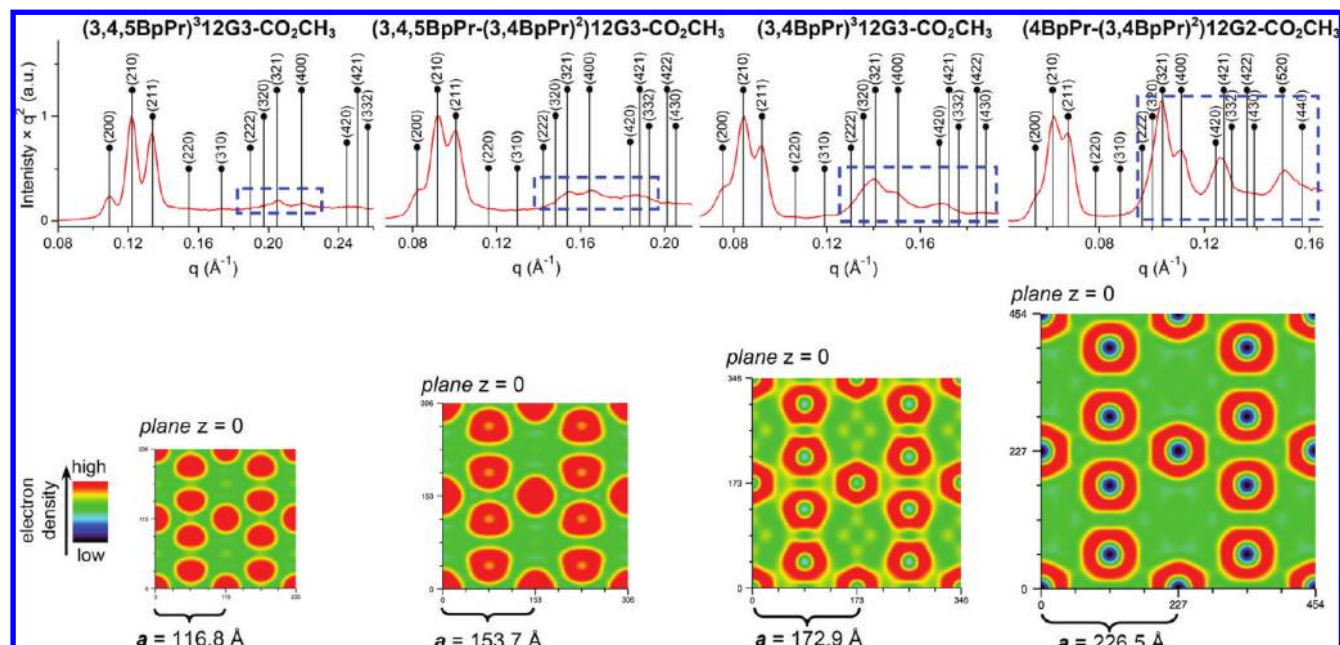


**Figure 6.** Small-angle powder XRD plots for selected BpPr dendrons that self-assemble into the  $Pm\bar{3}n$  cubic phase (top) and the corresponding reconstructed electron density maps, presented at relative scale (bottom). The dashed blue rectangles mark the increased intensity of the higher order diffraction peaks.

assembly was proposed wherein the dendrons adopt a conical conformation.<sup>4a</sup> TEM/ED<sup>33</sup> and XRD aided by isomorphous replacement<sup>34</sup> ultimately demonstrated that the  $Pm\bar{3}n$  cubic phase (*Cub*) was constructed from supramolecular micellar spheres. Oriented-fiber XRD experiments provided details of the internal structure of supramolecular dendrimers forming helical columns.<sup>10</sup> Due to the isotropic symmetry of the lattice, fiber XRD of cubic phases do provide less information on the internal structure of supramolecular dendrimers forming spheres. However, certain examples of biphenyl-4-methyl ether dendrons,<sup>19a</sup> AB<sub>4</sub> dendrons,<sup>17</sup> dendritic dipeptides,<sup>12</sup> and hybrid (AB)<sub>y</sub>-AB<sub>n</sub> dendrons self-assemble into supramolecular spheres exhibiting a chiral and hollow center. Recently, it was demonstrated that cyclotrimeratrylene (CTV)<sup>11</sup> and triphenylene (Tp)<sup>30</sup> functionalized with self-assembling benzyl ether dendrons exhibit a crown conformation that self-assembles into chiral spheres possessing a short internal helical arrangement.

In previous libraries<sup>4a,18,19a</sup> of self-assembling dendrons, the formation of spherical objects followed a conical packing mechanism. The increased molecular dimensions of dendrons constructed from BpPr building blocks make it possible to identify alternative mechanisms of spherical self-assembly. Four examples of BpPr dendrons with similar molecular dimensions that self-organize into the *Cub* phase that exhibit a sequential decrease in the observed lattice dimensions were chosen for further investigation (Figure 6). (3,4,5BpPr)<sup>3</sup>12G3-CO<sub>2</sub>CH<sub>3</sub> has the smallest lattice constant  $a = 115 \text{ \AA}$  ( $D = 73 \text{ \AA}$ ), increasing to  $a = 154 \text{ \AA}$  ( $D = 95 \text{ \AA}$ ) for (3,4,5BpPr-(3,4BpPr)<sup>2</sup>)12G3-CO<sub>2</sub>CH<sub>3</sub>,  $a = 173 \text{ \AA}$  ( $D = 107 \text{ \AA}$ ) for (3,4BpPr)<sup>3</sup>12G3-CO<sub>2</sub>CH<sub>3</sub>, and  $a = 227 \text{ \AA}$  ( $D = 140 \text{ \AA}$ ) for (4BpPr-(3,4BpPr)<sup>2</sup>)12G2-CO<sub>2</sub>CH<sub>3</sub>. With decreasing degree of branching, increased lattice dimensions are observed as well as more pronounced low electron density in the center of the supramolecular sphere

corresponding to an increased amplitude of higher order diffraction peaks (Figure 6).

In the conical packing model, the self-assembled sphere has a diameter that is approximately double the apex-to-periphery length ( $L$ ) of an individual cone-shaped dendron (Figure 7c). Recently, it has been demonstrated that in the *Cub* phase the compression<sup>31</sup> of the dodecyloxy tails is 31% at 110 °C, while the compression of the aromatic core is negligible. Additionally, it was shown that from 20 to 110 °C the relative compression of the alkyl tail increased by only 5%. Thus, it can be estimated that in *Cub* phases generated from BpPr dendrons the alkyl tails are compressed by 25–30% via chain melting. For the dendrons (3,4,5BpPr)<sup>2</sup>12G3-CO<sub>2</sub>CH<sub>3</sub>, (3,4,5BpPr-(3,4BpPr)<sup>2</sup>)12G3-CO<sub>2</sub>CH<sub>3</sub>, (3,4BpPr)<sup>3</sup>12G3-CO<sub>2</sub>CH<sub>3</sub>, and 4BpPr-(3,4BpPr)<sup>2</sup>12G2-CO<sub>2</sub>CH<sub>3</sub>, the apex-to-periphery length ( $L$ ) in the conical dendron conformation is  $\sim 50 \text{ \AA}$  (Figure 7a) for the all-*trans* conformation or closer to 45 Å for melted alkyl tails. Therefore, the expected diameter of the supramolecular spheres built from these molecules should be between 90 and 100 Å. For (3,4,5BpPr-(3,4BpPr)<sup>2</sup>)12G3-CO<sub>2</sub>CH<sub>3</sub> the experimentally determined diameter of 95 Å is in agreement with the expected size, 90–100 Å, of the spheres that would be obtained via the conical model of packing. (3,4BpPr)<sup>3</sup>12G3-CO<sub>2</sub>CH<sub>3</sub> has an experimentally determined spherical diameter of 107 Å which is close to, but slightly above, the expected size of the sphere and may indicate a small hollow center (Figure 7). This is corroborated by the increased amplitude of the higher order diffraction peaks obtained via SAXS, which were previously attributed to a low-electron density core region.<sup>12</sup> It is interesting to note that the biphenyl-4-methyl ester dendron of similar primary structure, (3,4BpPr)<sup>3</sup>12G3-CO<sub>2</sub>CH<sub>3</sub>,<sup>19a</sup> also exhibited experimental diameters that are 20 Å larger than the theoretically predicted diameter of a dendritic dimer.<sup>19a</sup> However, for (4BpPr-(3,4BpPr)<sup>2</sup>)12G2-CO<sub>2</sub>CH<sub>3</sub> the experimentally determined spherical diameter is 140 Å. This is suggestive of a large hollow center greater than 25 Å in diameter which is supported by a significant enhancement of the higher order diffraction peaks (Figure 7d). At the other extreme, (3,4,5BpPr)<sup>3</sup>12G3-CO<sub>2</sub>CH<sub>3</sub> has an experimentally

(33) Hudson, S. D.; Jung, H.-T.; Percec, V.; Cho, W.-D.; Johansson, G.; Ungar, G.; Balagurusamy, V. S. K. *Science* **1997**, *278*, 449–452.

(34) Dukeson, D. R.; Ungar, G.; Balagurusamy, V. S. K.; Percec, V.; Johansson, G. A.; Glodde, M. *J. Am. Chem. Soc.* **2003**, *125*, 1594–15980.

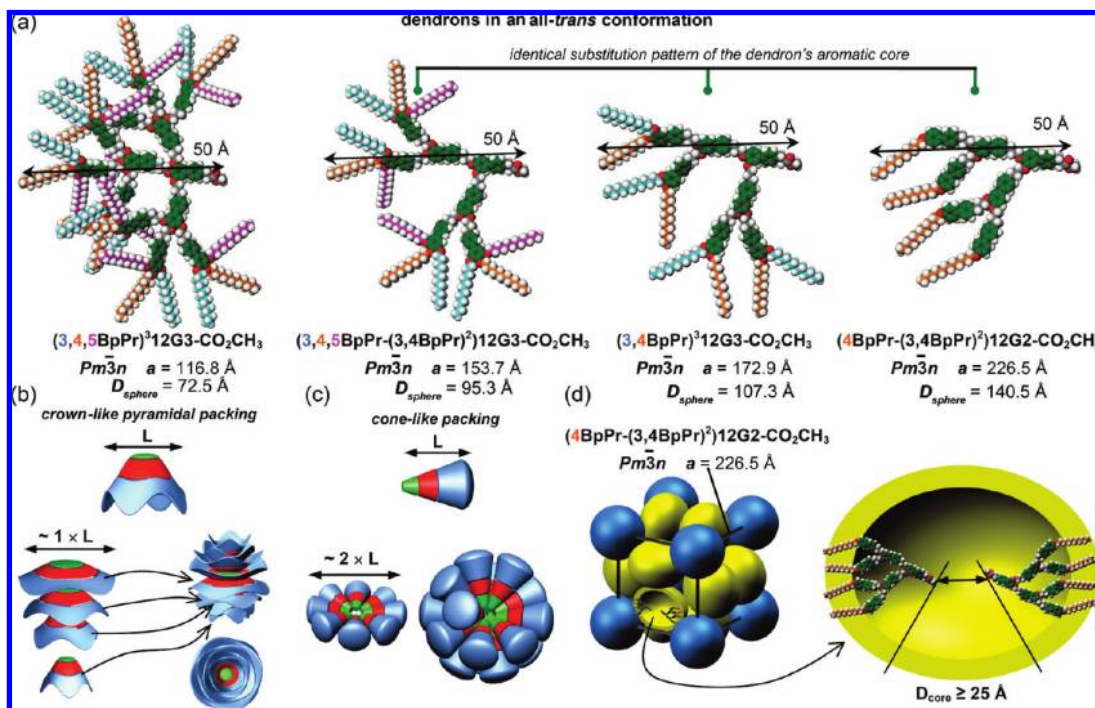


**Figure 7.** Molecular models of the four chosen dendrons in the all-trans conformation (a), crown-like pyramidal packing proposed for  $(3,4,5\text{BpPr})^3 12\text{G3-CO}_2\text{CH}_3$  (b), cone-like packing proposed for  $(3,4,5\text{BpPr-(3,4BpPr)}_2) 12\text{G3-CO}_2\text{CH}_3$  and  $(3,4\text{BpPr})^3 12\text{G3-CO}_2\text{CH}_3$  (c). Unit cell and to-scale molecular model of  $(4\text{BpPr-(3,4BpPr)}_2) 12\text{G2-CO}_2\text{CH}_3$  depicting the lower bound of the empty core diameter  $D_{\text{core}}$  (d).

determined diameter of 73 Å, and therefore it is ~23% smaller than expected for a conical-packing model assuming melted alkyl tails. For dendronized CTV<sup>11</sup> a crown conformation exists. For dendronized Tp<sup>30</sup> a model for the self-assembly of supramolecular spheres was discovered wherein the dendronized discs adopt a crown conformation. These dendritic crowns form spheres composed of short helical pyramidal columns that are spherically distorted. Therefore,  $(3,4,5\text{BpPr})^3 12\text{G3-CO}_2\text{CH}_3$  may adopt a crown conformation and pack into pyramidal helical spheres. Supramolecular spheres composed of dendritic crowns were not observed in previous libraries. However, due to the smaller dimensions of the dendrons and of the corresponding supramolecular spheres, it would not have been possible to distinguish between the various models.

Molecular topology controls the diameter of the supramolecular sphere. Comparison of all generation three BpPr dendritic esters and dendritic esters of similar molecular dimensions (e.g.,  $(4\text{BpPr-(3,4BpPr)}_2) 12\text{G2-CO}_2\text{CH}_3$ ) forming supramolecular spheres self-organized into Cub lattices shows that as the number of alkyl tails ( $x$ ) increases at the periphery, the diameter of the supramolecular sphere and the number of dendrons required to generate the sphere decrease (Figure 8, left). Additionally, examination of the projection of the solid angle ( $\alpha'$ ) demonstrates a roughly linear increase of the effective molecular taper angle with increasing number of alkyl tails (Figure 8, right). The  $\alpha'$  of hollow, vesicular, or crown-like spheres, which interestingly exist only for the lowest or highest number of alkyl tails, are calculated in the same manner as that for conical spheres and may not be accurate. Dendritic alcohols were not included in this analysis, as H-bonding interactions will result in spherical compression. This trend is not as clear if the aliphatic weight fraction of the dendron is used as the structural variable. Interestingly, only for 4–6 alkyl tails per dendron do both columnar and spherical structures form at different temperature ranges. Likewise only for 4 alkyl tails does a substantial

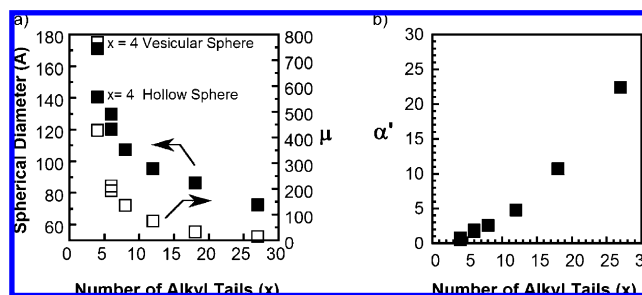


**Figure 8.** Effect the number of alkyl tails ( $x$ ) on the spherical diameter and on the number of dendrons per supramolecular dendritic sphere ( $\mu$ ) generated from third generation dendrons or dendrons of comparable molecular dimensions (a). Dependence of the calculated projection of the solid angle ( $\alpha'$ ) of the dendrons in the supramolecular sphere on the number of alkyl tails ( $x$ ) (b).

hollow center become apparent for  $(4\text{BpPr-(3,4BpPr)}_2) 12\text{G2-CO}_2\text{CH}_3$  or a giant vesicular sphere is observed for the constitutional isomer  $(4\text{BpPr-3,4BpPr-3,5BpPr}) 12\text{G2-CO}_2\text{CH}_3$ . Thus, the number of alkyl tails at the dendron periphery can be employed as a design element to tailor the shape and also to determine the diameter of the spherical supramolecular dendrimers, number, and conformation of dendrons from which they are generated.

**Ultra-high Molecular Weight Supramolecular Spheres via an Unprecedented Interdigitated Vesicular Self-Assembly.** In the previous section, it was demonstrated that the increased diameter of the supramolecular dendrimers generated from BpPr dendrons allowed for the distinction between various modes of spherical self-assembly. The previous examples showed that decreasing the degree of branching in dendrons that form supramolecular spheres results in a progressive increase in the diameter of the supramolecular sphere and a concomitant decrease in the electron density at the center of the sphere. At the extreme, a large hollow center was proposed for  $(4\text{BpPr-}$

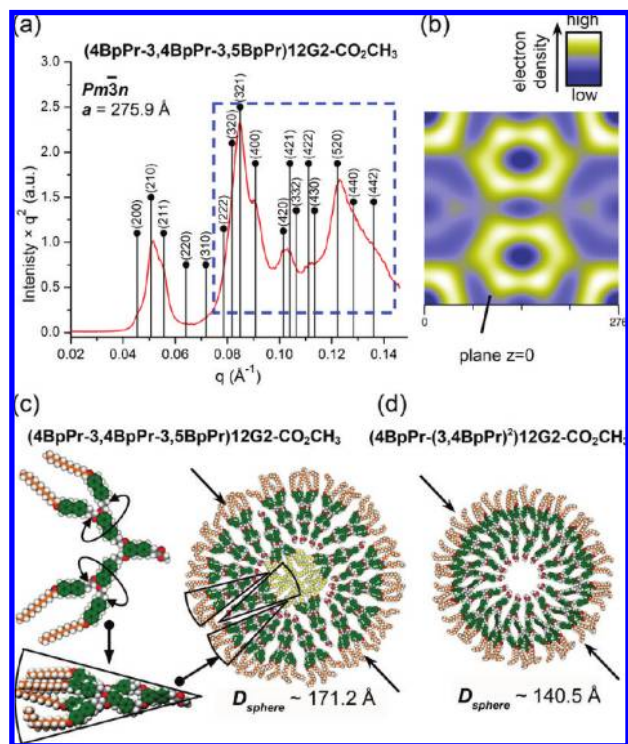


**Figure 9.** Vesicular cubic phase: (4BpPr-3,4BpPr-3,5BpPr) $_{12}$ G $_{2}$ -CO $_{2}$ CH $_{3}$  XRD powder plot with the increased relative intensities of the high order peaks marked by the dotted rectangle (a), corresponding relative electron density map (b), corresponding model of the self-assembled vesicular sphere (c), and comparison with the model of the hollow cubic spheres self-assembled from (4BPb-(3,4BPb) $_{2}$ ) $_{12}$ G $_{2}$ -CO $_{2}$ CH $_{3}$  (d).

(3,4BpPr) $_{2}$ ) $_{12}$ G $_{2}$ -CO $_{2}$ CH $_{3}$ . The constitutional isomer of (4BpPr-(3,4BpPr) $_{2}$ ) $_{12}$ G $_{2}$ -CO $_{2}$ CH $_{3}$  resulting from a change in the apex branching unit, (4BpPr-3,4BpPr-3,5BpPr) $_{12}$ G $_{2}$ -CO $_{2}$ CH $_{3}$ , exhibits an even larger experimental diameter of 171.2 Å. Reconstructed electron density maps demonstrated a low-electron density at the center of the sphere which could indicate a hollow center. However, this hollow center would have a diameter of 70–80 Å or over 40% of the total spherical diameter and is unrealistic for self-organized soft-condensed matter. Additionally, while there may be a small cavity at the center of the vesicular sphere, the electron density of the interior does not appear low-enough to support an entirely empty core. Therefore, an alternative interdigitated vesicular model of spherical self-assembly was proposed to explain this structure (Figure 9). The improved conformational flexibility of the 3,5-branching unit at the apex allows compression of the molecular taper angle  $\alpha'$  thereby permitting interdigitation of narrow wedges to form a bilayer structure. As expected for the vesicular model, conversion of (4BpPr-3,4BpPr-3,5BpPr) $_{12}$ G $_{2}$ -CO $_{2}$ CH $_{3}$  to the corresponding alcohol completely destabilizes the vesicular phase resulting in  $\Phi_{r-c}$  self-organization. As the vesicular structure contains two layers of dendrons, an extraordinarily high number of dendrons compose each sphere. The supramolecular sphere composed of 770 *quasi-equivalent* building blocks has a molecular weight of  $1.73 \times 10^6$  g/mol. The largest  $\mu$  value previously encountered for supramolecular dendritic spheres self-organized into a *Cub* lattice was 191, for (4Pr-(3,4Pr) $_{2}$ ) $_{12}$ G $_{2}$ -CO $_{2}$ CH $_{3}$ , with a corresponding molecular weight for the supramolecular dendrimer of  $3.41 \times 10^5$  g/mol.<sup>18</sup> Thus, this new example represents an  $\sim 4$ -fold increase in  $\mu$  and a 5-fold increase in mass, achieving the first supramolecular dendrimer with an

ultrahigh molecular weight (MW  $\geq 1.0 \times 10^6$  g/mol). For the biphenyl-4-methyl ether dendron (3,4Bp) $_{2}$ ) $_{12}$ G $_{2}$ -CO $_{2}$ C $_{4}$ H $_9$ ,  $\mu = 243$  and MW =  $3.30 \times 10^5$  g/mol and for (4Bp-3,4Bp-3,5Bp) $_{12}$ G $_{2}$ -CO $_{2}$ CH $_{3}$ , a dendron of similar primary structure to the current example,  $\mu = 261$  and  $M_w = 5.34 \times 10^5$  g/mol.<sup>19a</sup> While it was not apparent at the time, these biphenyl-4-methyl ether dendrons with high  $\mu$  values may also be examples of the interdigitated vesicular cubic phase. There too, the vesicular phase was disrupted by conversion of the apex group to an alcohol.

This vesicular spherical supramolecular dendrimer is of the dimensions, shape, and mass comparable only to those of the most complex biological assemblies such as eukaryotic ribosomes, which weigh approximately  $2.5 \times 10^6$  g/mol.<sup>35</sup> As the size of supramolecular dendrimers approaches the wavelength of visible light, the periodic variation in the electron density between the aliphatic and aromatic domains will provide an entry into optoelectronic materials. Achieving such sizes via a traditional conical packing mechanism would require self-assembling dendrons that are extremely long which therefore must be prepared from very high generation dendrons. This would also need to exhibit an extremely small molecular taper angle and limited branching. Through interdigitation and multilayer packing, vesicular spheres may achieve this goal with significantly smaller and synthetically more feasible dendrons. Additionally, dendritic macromonomers that form self-assembling spheres of this size may also provide a route to monodisperse ultrahigh molecular weight polymers through the self-interruption of their polymerization process.<sup>36</sup>

**Helical Porous and Nonporous Columns Exhibiting Intracolumnar Order.** The self-organization of arylether dendrons into  $\Phi_h$  lattices generated from helical porous columns was first observed with self-assembling dendritic dipeptides.<sup>14</sup> In addition to larger than expected  $D_{col}$  for filled columns, hollow columns also showed characteristic enhancement of higher-order 110, 200, and 210 diffraction peaks. Recently, helical porous supramolecular columns were also observed in libraries of phenylpropyl<sup>18</sup> and biphenyl-4-methyl ether<sup>19a</sup> and in libraries of dendrons with a more complex architecture<sup>19b</sup> that did not contain a dipeptide as the apex group. The helical diffraction theory of Cochran, Crick, and Vand<sup>9</sup> was recently adapted for the analysis of helical supramolecular dendrimers.<sup>10,17,37</sup>

In spite of the twisted conformation of the two phenyl units forming the biphenyl group, many BpPr dendrons self-organize into  $\Phi_h$  lattices possessing internal helical order and hollow centers. The representative XRD data, the column ( $D_{col}$ ) and pore ( $D_{pore}$ ) diameters of helical supramolecular columns self-organized in the  $\Phi_h$  phase, are presented in Table 4. (4BpPr-(3,4BpPr) $_{2}$ ) $_{12}$ G $_{2}$ -CO $_{2}$ CH $_{3}$  exhibits the largest  $D_{pore}$  ( $16.7 \pm 2.6$  Å). (4BpPr-(3,4BpPr) $_{2}$ ) $_{12}$ G $_{2}$ -CO $_{2}$ CH $_{3}$  also exhibits a high temperature *Cub* phase with a hollow center, indicating that primary structures favoring hollow columns may also favor hollow spherical self-assembly. The corresponding alcohol, (4BpPr-(3,4BpPr) $_{2}$ ) $_{12}$ G $_{2}$ -CH $_2$ OH, forms a hollow helical column with a smaller  $D_{pore}$  ( $12.5 \pm 2.0$  Å). A decreased diameter of the hollow center was also observed in the higher temperature *Cub* phase and was attributed to the H-bonding interactions of the apex group. Retrostructural analysis and Cerius2 simulation

(35) Ramakrishnan, V.; Moore, P. B. *Curr. Opin. Struct. Biol.* **2001**, *11*, 144–154.

(36) Percec, V.; Ahn, C.-H.; Barboiu, B. *J. Am. Chem. Soc.* **1997**, *119*, 12978–12979.

(37) Peterca, M.; Percec, V.; Dulcey, A. E.; Nummelin, S.; Korey, S.; Ilies, M.; Heiney, P. A. *J. Am. Chem. Soc.* **2006**, *128*, 6713–6720.

**Table 4.** Measured and Fitted XRD Peak Amplitudes, Column, and Pore Diameter for BpPr Dendrons forming Hollow Helical Supramolecular Dendrimers that Self-Organize into  $\Phi_h$  Lattices

dendrion	$T$ ( $^{\circ}\text{C}$ )	$q_{10}^a$ ( $\text{\AA}^{-1}$ ) [ $A_{10}$ , $A_{10}$ ] <sup>b</sup> (a.u., a.u.)	$q_{11}^a$ ( $\text{\AA}^{-1}$ ) [ $A_{11}$ , $A_{11}$ ] <sup>b</sup> (a.u., a.u.)	$q_{20}^a$ ( $\text{\AA}^{-1}$ ) [ $A_{20}$ , $A_{20}$ ] <sup>b</sup> (a.u., a.u.)	$q_{21}^a$ ( $\text{\AA}^{-1}$ ) [ $A_{21}$ , $A_{21}$ ] <sup>b</sup> (a.u., a.u.)	$D_{\text{colmeas}}$ , $D_{\text{colfit}}$ <sup>c</sup> ( $\text{\AA}$ )	$D_{\text{pore}}^d$ ( $\text{\AA}$ )
(4BpPr-3,4BpPr-3,4,5BpPr)12G2-CH <sub>2</sub> OH	30	0.0865 [41.50, 42.45]	0.1499 [25.13, 27.16]	0.1731 [21.79, 18.11]	0.2289 [8.80, 7.12]	41.6, 42.2	12.4 $\pm$ 2.2
(4BpPr-(3,4BpPr) <sup>2</sup> )12G2-CO <sub>2</sub> CH <sub>3</sub>	135	0.0740 [34.23, 35.81]	0.1282 [24.56, 28.36]	0.1480 [23.03, 20.30]	0.1958 [6.70, 6.03]	46.9, 47.0	16.7 $\pm$ 2.6
(4BpPr-(3,4BpPr) <sup>2</sup> )12G2-CH <sub>2</sub> OH	125	0.0810 [42.72, 43.81]	0.1403 [26.30, 28.18]	0.1620 [21.43, 18.06]	0.2143 [6.12, 5.04]	44.7, 44.9	12.5 $\pm$ 2.0
(4BpPr-3,4,5BpPr-3,5BpPr)12G2-CO <sub>2</sub> CH <sub>3</sub>	140	0.0845 [40.74, 41.50]	0.1463 [26.13, 27.59]	0.1690 [23.85, 19.09]	0.2235 [7.36, 6.37]	42.3, 42.0	13.8 $\pm$ 2.0
(4BpPr-3,4,5BpPr-3,5BpPr)12G2-CH <sub>2</sub> OH	150	0.0896 [41.28, 42.36]	0.1551 [25.61, 28.20]	0.1791 [21.88, 16.82]	0.2370 [7.83, 6.35]	40.8, 40.8	11.5 $\pm$ 2.0

<sup>a</sup>  $q_{hk}$  =  $hk$  diffraction peak position. <sup>b</sup> [ $A_{hk}$ ,  $A_{hk}$ ] = measured and fitted ( $hk$ ) diffraction peak amplitude, a.u. = arbitrary units. <sup>c</sup>  $D_{\text{colmeas}}$  = measured column diameter,  $D_{\text{colfit}}$  = fitted column diameter. <sup>d</sup>  $D_{\text{pore}}$  = calculated pore diameter.

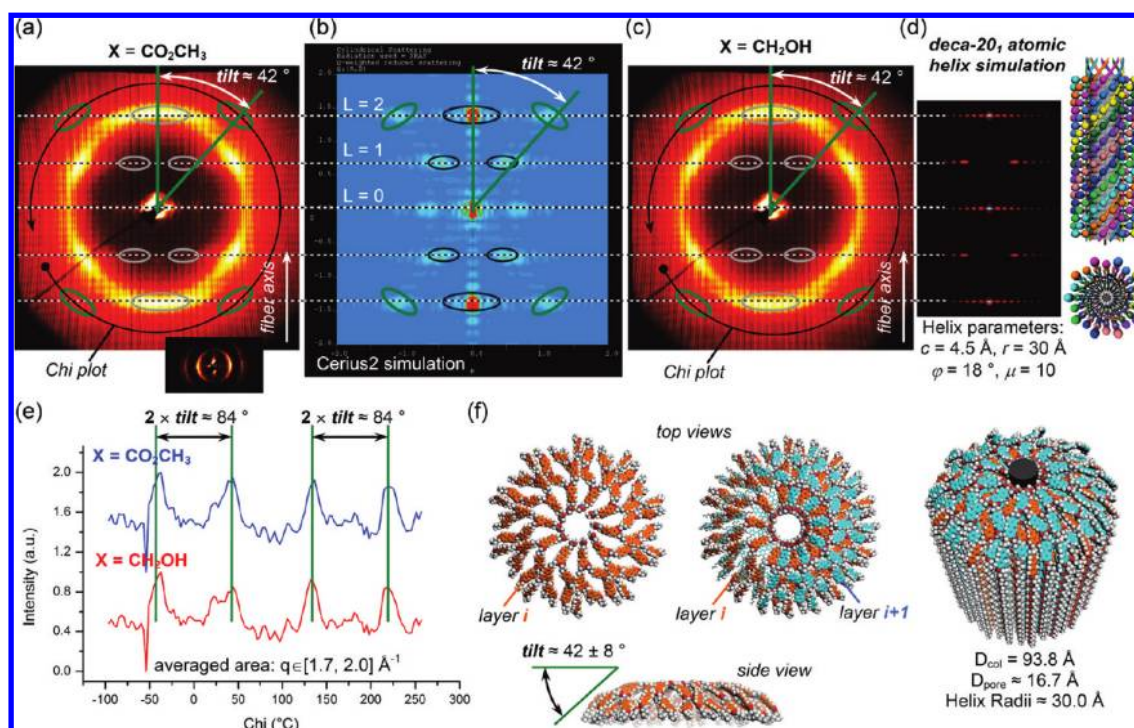


**Figure 10.** Supramolecular crown conformations assembled from (4BpPr-(3,4BpPr)<sup>2</sup>)-12G2-X (X = CO<sub>2</sub>CH<sub>3</sub> and CH<sub>2</sub>OH) and their self-organization into helical pyramidal columns. Wide-angle XRD oriented fiber patterns collected at 25  $^{\circ}\text{C}$  for X = CO<sub>2</sub>CH<sub>3</sub> (a), compared with the Cerius2 simulated diffraction pattern based on the corresponding molecular models of (4BpPr-(3,4BpPr)<sup>2</sup>)-12G2-CO<sub>2</sub>CH<sub>3</sub> (b), wide-angle XRD oriented fiber pattern collected at 25  $^{\circ}\text{C}$  for X = CH<sub>2</sub>OH (c), and theoretical diffraction pattern for a deca-20<sub>1</sub> helix (d). Azimuthal Chi angle plots along the region indicated on the fiber patterns (e). Molecular model for the X = CO<sub>2</sub>CH<sub>3</sub> (f). In (a, c): L indicates helical layer line; tilt indicates dendron tilt angle or tilt correlation features (marked in green); long-range helical features are marked by the gray colored circles.

of the diffraction pattern of the modeled hollow helical columns formed from (4BpPr-(3,4BpPr)<sup>2</sup>)-12G2-X suggest self-assembly into supramolecular crowns that form a novel *deca-20*<sub>1</sub> atomic helix (Figure 10). (4BpPr-3,4,5BpPr)12G1-CH<sub>2</sub>OH also self-assembles into supramolecular crowns that form a novel *octa-16*<sub>1</sub>-atomic helix but, in contrast to the previous example, does not exhibit a hollow center.

**A “Nanoperiodic Table” of Supramolecular Dendrimers.** The first self-assembling dendrons were designed to mimic the shape of the capsid protein of the tobacco-mosaic virus (TMV).<sup>38</sup> Later, it was shown that changes to the primary structure of dendrons result in different self-assembled supramolecular

structures and corresponding self-organized periodic lattices and quasi-periodic arrays.<sup>4</sup> Following the elaboration of libraries of benzyl ether self-assembling dendrons, a larger library of phenylpropyl ether self-assembling dendrons was prepared and analyzed.<sup>18</sup> Phenylpropyl ether dendrons replicated all the structures and lattices observed for the benzyl ether series except for the BCC lattice. Due to limited solubility only a smaller library of biphenyl-4-methyl ether self-assembling dendrons was reported.<sup>19a</sup> Comparison of the first three libraries of self-assembling dendrons suggest that the primary structure and not the type of building block employed had the most profound effect on the supramolecular structure. The BpPr self-assembling dendrons reported here allow for a more complete comparison between benzyl, phenylpropyl, biphenyl-4-methyl ether and BpPr self-assembling dendrons.

(38) (a) Percec, V.; Heck, J.; Lee, M.; Ungar, G.; Alvarez-Castillo, E. J. *Mater. Chem.* **1992**, *2*, 1033–1039. (b) Klug, A. *Angew. Chem., Int. Ed. Engl.* **1982**, *22*, 565–582.

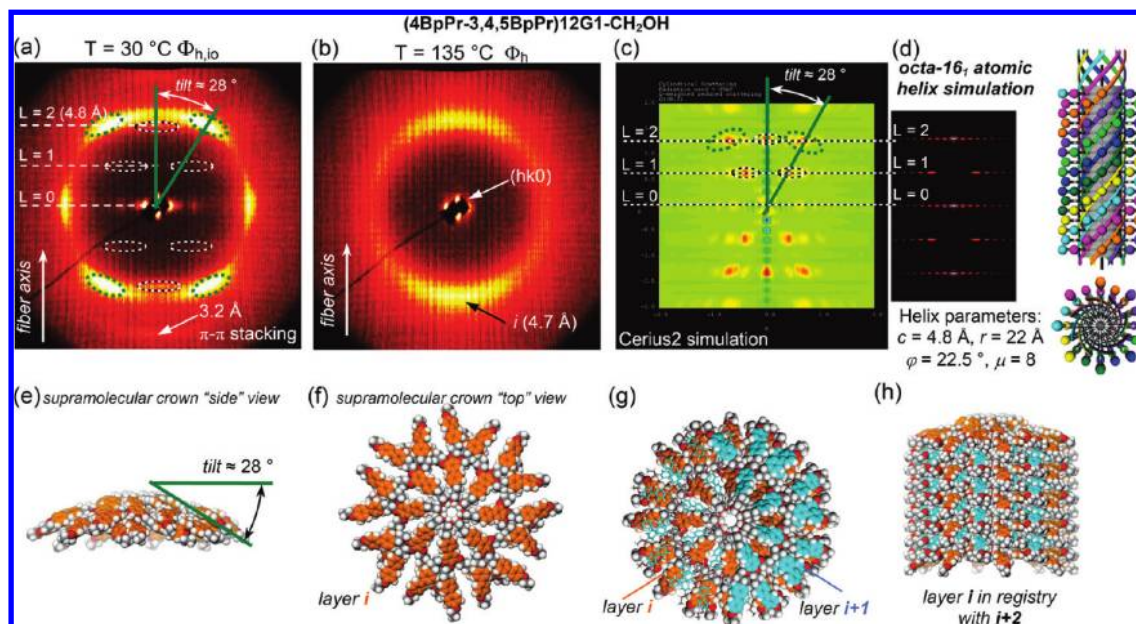


**Figure 11.** Wide-angle oriented fiber XRD patterns of the supramolecular columns assembled from the dendritic alcohol (4BpPr-3,4,5BpPr)12G1-CH<sub>2</sub>OH collected in the  $\Phi_{h,lo}$  phase (a) and  $\Phi_h$  phase (b). Cerius2 molecular model based simulation of the XRD pattern of the oriented fiber (c). Atomic helical packing, helix parameters, and the corresponding simulated XRD pattern (d) of the same supramolecular assembly. The molecular model of the supramolecular structure generated from (4BpPr-3,4,5BpPr)12G1-CH<sub>2</sub>OH used in the Cerius2 simulation (e, f, g, h).

Generally, the crystal structure of a molecule cannot be predicted *de novo*.<sup>39</sup> In certain systems such as linear diblock copolymers, self-assembly into microphase segregated structures can be predicted by the molar mass of the polymer, the immiscibility of the two blocks, and the weight fraction of the major and minor blocks. Structures prepared via AB diblock copolymers are architecturally similar to those accessible via self-assembling dendrons, such as spherical, hexagonal columnar, and lamellar structures which are observed in that order with increasing percentage of the minority block. However, for specific primary structures of dendrons the retention of supramolecular columns has been demonstrated for 10 to 57% of the aliphatic weight fraction,<sup>14b</sup> and likewise supramolecular spheres are persistent from 40 to 84% of the aliphatic weight fraction.<sup>34</sup> Additionally, numerous examples of constitutional isomeric dendrons with the same aliphatic/aromatic weight ratio self-assemble into completely different structures. Therefore, it is not the weight fraction but rather the molecular topology that most profoundly influences the tertiary structure of supramolecular dendrimers.

The tertiary structure of self-assembled dendrons is determined by the molecular topology or its primary structure. Therefore, analysis of the sequence–structure relationship is more appropriately handled via methods used in structural biology. A widely applied technique for the prediction of a protein's tertiary structure from its primary structure is to identify proteins of similar primary structure for which a tertiary structure has been determined. The more similar the primary structures, the more likely it is that they will adopt a similar tertiary structure. Figures 12, 13, and 14 summarize the tertiary and quaternary structures formed for similar primary structures but using different dendritic building blocks.<sup>4,18,19</sup> They provide a 'nanoperiodic table'<sup>20</sup> of supramolecular dendrimers that

demonstrates general trends in the sequence–structure relationship and identifies clustered regions where specific structures can be found. The supramolecular structures formed can be classified as lamellar, columnar, or spherical in analogy to the  $\beta$ -sheet and helical structures of fibrillar proteins and the pseudospherical structure of globular proteins.

For all three libraries, the generation one dendrons are the same and exhibit a high proportion of lamellar and columnar structures, including hollow columnar structures. In fact only (3,4,5)12G1CO<sub>2</sub>M, where M is a metal cation, form spherical supramolecular dendrimers (Figure 12). The 3,4,5-library (Figure 12) progresses rapidly to predominantly spherical structures at generation three and entirely spherical structures from generation three through five. The spherical supramolecular dendrimers mostly pack into Cub lattices. Sporadic examples of packing into QLC arrays can be found at generation two and three in the 3,4,5-library. At generation one, the columnar structures form a roughly even mixture of  $\Phi_h$ ,  $\Phi_{r-s}$ , and  $\Phi_{r-c}$  lattices. At generation two, columnar structures pack almost exclusively into the  $\Phi_h$  lattice. The primary structure (4-3,4-3,4,5) is biased toward the formation of porous columns.

The 3,4-library (Figure 13) contains the same generation one dendrons as the 3,4,5-library. At generation two, the 3,4-library is similar to the 3,4,5-library, forming mostly spherical and hollow spherical structures. At generation two, the 3,4-library differs, containing lamellar, unknown, and more hollow columnar structures clustered around the (4-(3,4)<sup>2</sup>)12G2 primary structure. At generation three and four, only spherical structures are observed. As with the 3,4,5-library most of the spherical supramolecular dendrimers form Cub lattices. However, examples of QLC arrays and Tet lattices can be found for (3,4,5Pr-(3,4Pr)<sup>2</sup>)12G3-CH<sub>2</sub>OH and (3,4,5Pr-(3,4Pr)<sup>2</sup>)12G3-CO<sub>2</sub>H, respectively. The columnar lattices observed for generation two dendrons are biased toward  $\Phi_h$  self-organization, though for the (3,4)<sup>2</sup>12G2 primary structure there is a complete preference for  $\Phi_{r-c}$  self-organization.

(39) (a) Gavezzotti, A. *Acc. Chem. Res.* **1994**, *27*, 309–314. (b) Dunitz, J. D. *Chem. Commun.* **2003**, 545–548. (c) Dunitz, J. D.; Gavezzotti, A. *Angew. Chem., Int. Ed.* **2005**, *44*, 1766–1787.

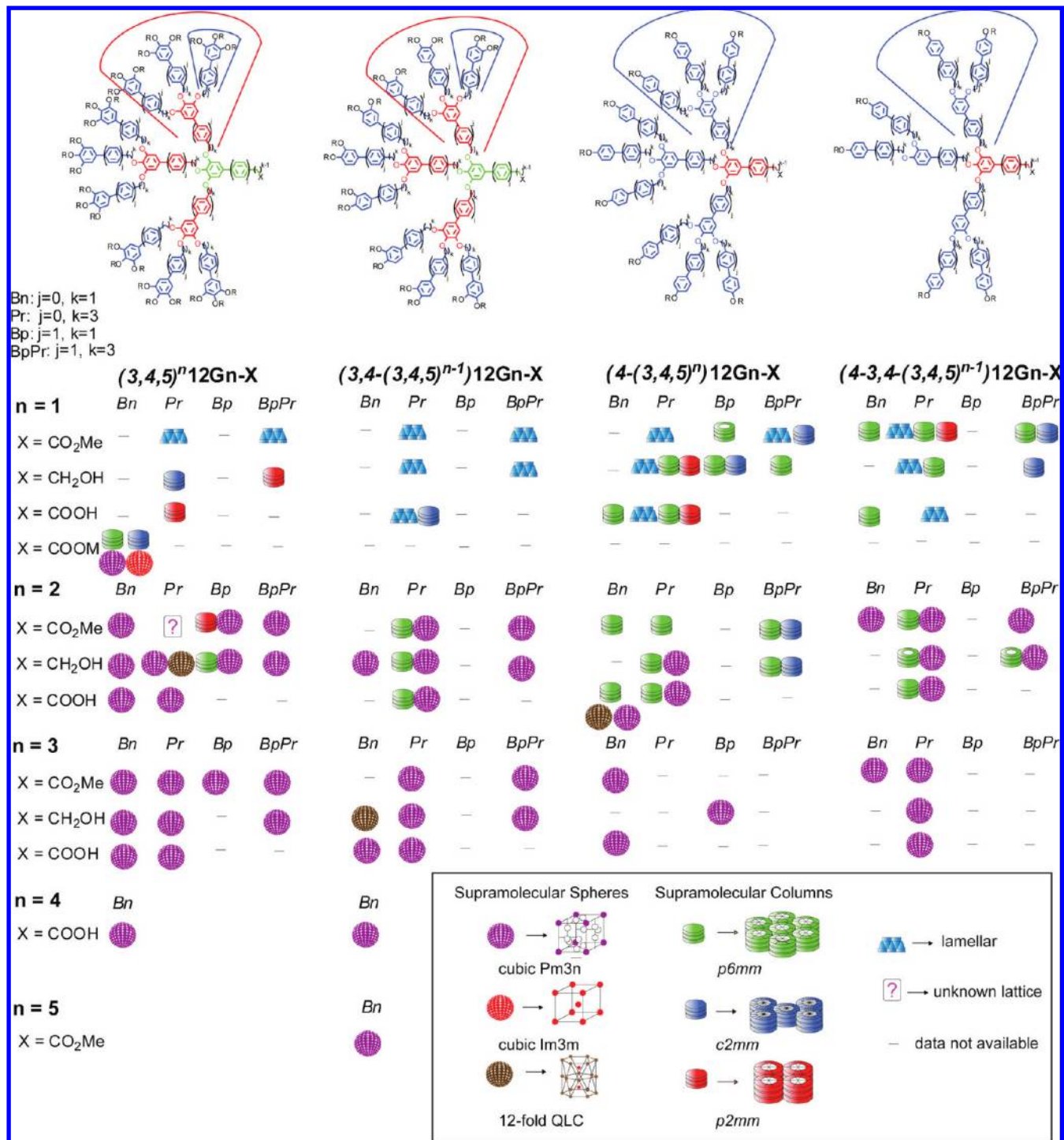


**Figure 12.** Primary structure vs 3D supramolecular structure for all libraries of AB<sub>3</sub> supramolecular dendrimers. Bn = benzyl ether, Pr = phenylpropyl ether, Bp = biphenyl-4-methyl ether, BpPr = biphenylpropyl ether.

The 3,5-library (Figure 14) exhibits a greater degree of architectural polymorphism than the 3,4- and 3,4,5-libraries. Generation two dendrons from the 3,5-libraries have a far higher propensity to form lamellar structures than the other libraries. The columnar structures formed from generation two dendrons in the 3,5-library exhibit mostly  $\Phi_h$  lattices, many containing a hollow center. Unlike, the 3,4- and 3,4,5-libraries very few spherical structures are observed for generation two dendrons in the 3,5-library. The propensity for columnar self-organization in the 3,5-library carries into the third and fourth generations. Unlike, the 3,4- and 3,4,5-libraries which form only spherical

structures at the third generation, generation three dendrons in the 3,5-library exhibit a nearly even mix of columnar and spherical, as well as a few lamellar, structures. The columnar structures formed by the generation three dendrons, self-organize almost exclusively into  $\Phi_h$  lattices. Many of the columnar structures are porous, specifically generation two and above dendrons with sequences  $(3,4-(3,5)^{n-1})12\text{Gn}$ ,  $(4-3,4,5-(3,5)^{n-2})12\text{Gn}$  and  $(4-3,4-(3,5)^{n-2})12\text{Gn}$ . The spherical structures formed by the generation three dendrons in the 3,5-library on the other hand do not generally self-organize into the otherwise ubiquitous  $Pm3n$  lattice but rather pack mostly into *Tet* and *QLC* lattices.

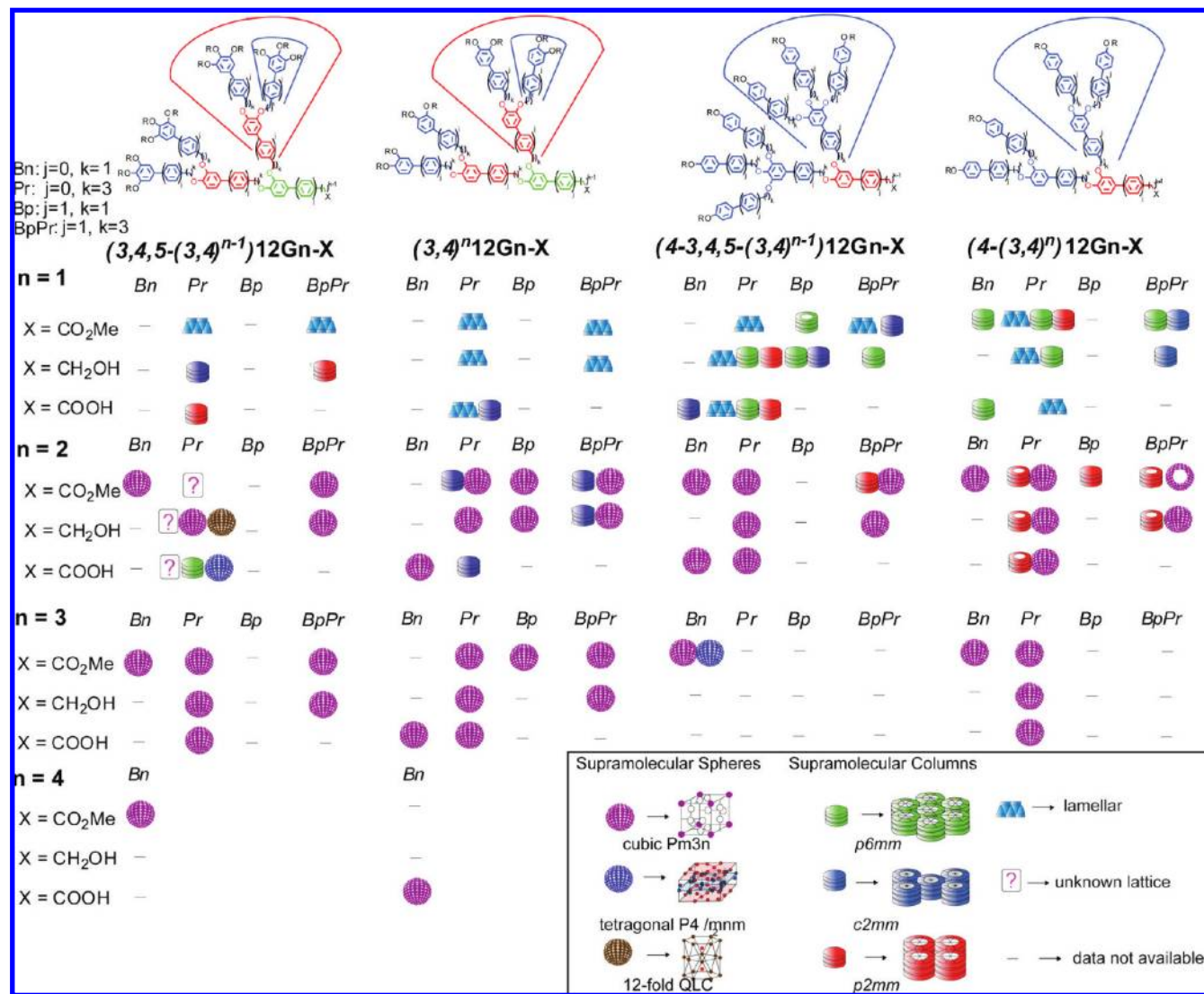


**Figure 13.** Primary structure vs 3D supramolecular structure relationship for all 3,4-disubstituted libraries of AB<sub>2</sub> supramolecular dendrimers. Bn = benzyl ether, Pr = phenylpropyl ether, Bp = biphenyl-4-methyl ether, BpPr = biphenylpropyl ether.

The high degree of architectural polymorphism in the 3,5-library is likely due to the greater flexibility of the 3,5-branching pattern caused by diminished steric effects. The decreased steric crowding also contributes to the ability of 3,5-branched dendrons to form columnar and lamellar structures that likely result from a highly planar wedge-like conformation of the dendron. This flexibility may also contribute to the tendency to pack into noncubic lattices of spherical supramolecular dendrimers at higher generation.

For all libraries, it is observed that, for a given primary structure, changes in apex functionality rarely perturb the type of structure formed or the corresponding lattice. However, it should be noted that changing the apex group from a non-H-bonding ester to an H-bonding alcohol or carboxylic acid will result in decreased object size, increased phase transition temperatures, and partial or complete elimination of pores. In rare examples such as the new vesicular cubic phase observed for (4BpPr-3,4BpPr-3,5BpPr)12G2-CO<sub>2</sub>CH<sub>3</sub>, alteration of the apex group from an ester to alcohol completely changes the shape of the supramolecular dendrimer from a sphere to a column or vice versa. It is also observed that, for a given branching pattern and apex groups, changes to the type of

building block, i.e. benzyl, phenylpropyl, biphenyl-4-methyl, or biphenylpropyl ether, do not significantly alter the type of supramolecular objects formed. The limited effect of the apex group or building block type on the self-assembled structure is an indication that it is shape recognition, rather than directed interactions, that most strongly influences self-assembly and self-organization.

Not all primary structures were produced for every class of building block and some primary structures adopt different supramolecular structures at different temperatures. However, analysis of the data presented in Figures 12, 13, and 14 demonstrate an 82% predictability, defined here as the percentage of similar primary structures resulting in at least one conserved supramolecular shape. Thus, only 18% of similar primary structures produce completely distinct sets of supramolecular shapes. Predictability is largely unchanged in the full analysis of all four libraries or subsets two or three libraries. It is worth noting that the AB<sub>3</sub> and 3,4-disubstituted AB<sub>2</sub> libraries alone exhibited 5% greater predictability than the 3,5-disubstituted AB<sub>2</sub> library. More importantly, it is noted that predictability increases from 73% at generation one to 77% at generation two to 95% at generation three. Thus, the higher the generation

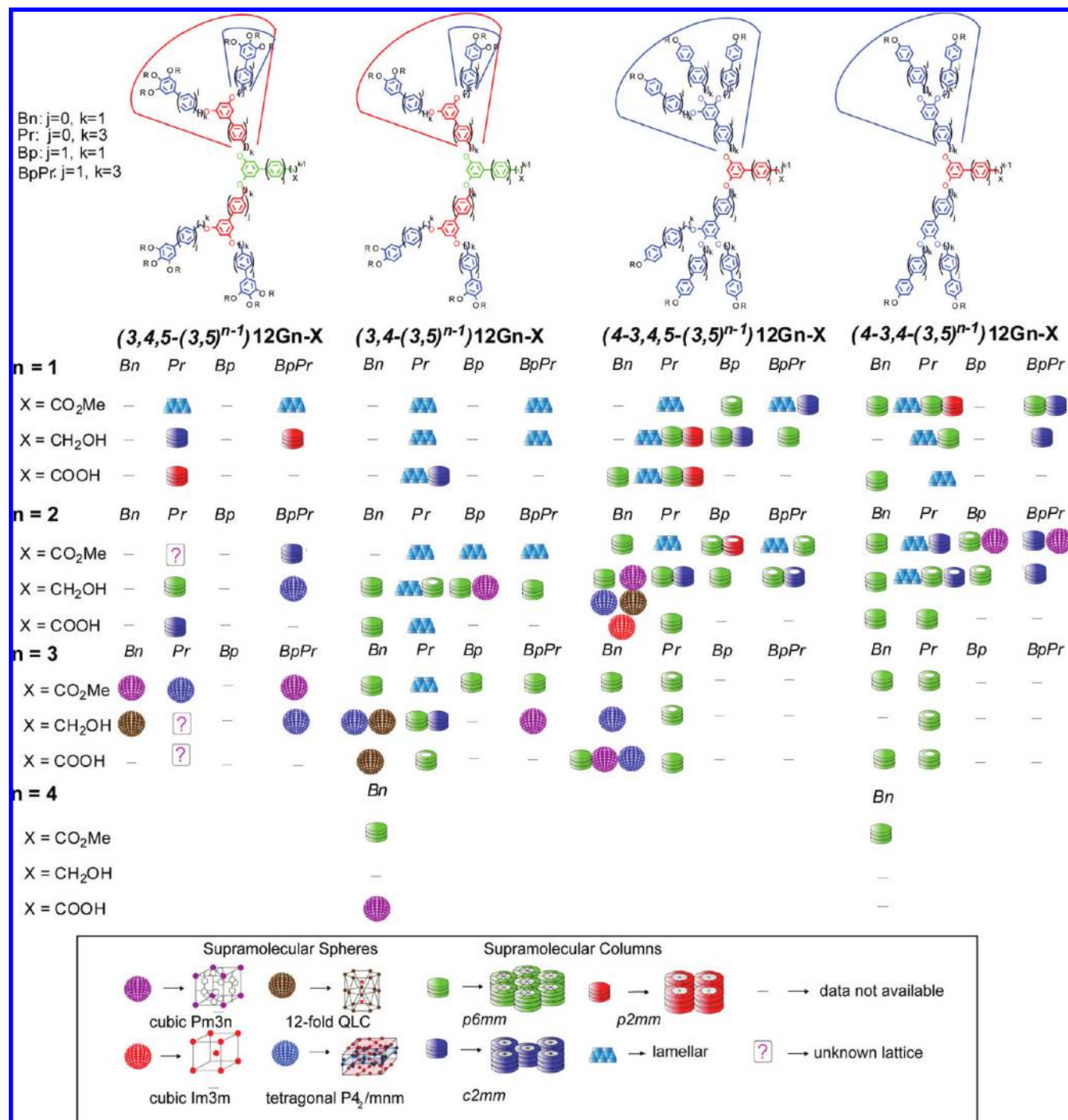


**Figure 14.** Primary structure vs 3D supramolecular structure for all 3,5-disubstituted libraries of AB<sub>2</sub> supramolecular dendrimers. Bn = benzyl ether, Pr = phenylpropyl ether, Bp = biphenyl-4-methyl ether, BpPr = biphenylpropyl ether.

dendron and thus the more synthetic effort required, the higher the chance that a new dendron will adopt the targeted supramolecular structure. To more accurately quantify the relationship between elements of the primary structure and the corresponding tertiary structure, a queryable database of self-assembling dendrimers elaborated in our laboratory depicted in Figures 12, 13, and 14 as well as other hybrid-dendrons<sup>4c,19b</sup> was constructed. Using this database, it was determined that dendrons with the same branching pattern, same type of building block, but different apex group exhibit at least one phase composed of the same shape of supramolecular dendrimer 83% of the time. Dendrons with the same branching pattern, same apex group,

but different type of building block exhibit at least one phase composed of the same shape of supramolecular dendrimer 81% percent of the time. However, dendrons with the same building block, same apex group, but different primary structures produce completely different shaped supramolecular dendrimers 47% of the time. A single change in the branching pattern results in the largest decrease in structural retention from 100% to ~60%, though sequential changes result in a continual decrease in the likelihood of a conserved structure.

Through both qualitative and quantitative analysis, it is evident that the shape of the supramolecular dendrimer is determined largely by the primary structure of the dendron, and

not the type of building block or apex group. In proteins the primary structure which is the linear sequence of amino acids determines the secondary, local 3D, and tertiary, global 3D, structure.<sup>40</sup> The tolerance of a protein sequence to point mutation of specific residues is complex. In some cases the folded structure and corresponding function are retained, while other residues are more critical and their modification results in a different fold or function. In self-assembling aryl ether dendrons, the primary structure corresponds to nonlinear connectivity, and therefore, a single mutation to the primary structure results in a more drastic change to the molecular topology and, therefore, to the tertiary structure. The tendency of self-assembling dendrons to retain a 3D supramolecular structure despite homologation of the building block mimics the relationship of synthetic  $\beta$ - and  $\gamma$ -amino acids to the natural  $\alpha$ -amino acids.<sup>41</sup> Polypeptides derived from  $\alpha$ -,  $\beta$ -, and  $\gamma$ -amino acids form generally similar helical and sheet-like structures as well as structural motifs that comprise globular proteins, but due to backbone elongation and different spatial arrangements of H-bond donors and acceptors, specific features vary.

While the development of a 'nanoperiodic table' for self-assembling supramolecular aryl ether dendrons will allow for the design of new molecules with tailored shapes and properties, the synthesis of libraries of self-assembling dendrons is a powerful tool for discovery and most probably applies to other building blocks. It remains to be seen whether a similar strategy of library synthesis can be applied to other classes of self-assembling dendrons constructed from chemically dissimilar subunits<sup>5</sup> and whether that will reveal a relationship between primary, tertiary, and quaternary structures.

## Conclusions

The synthesis and retrostructural analysis of three libraries of AB<sub>3</sub> and constitutional isomeric AB<sub>2</sub> self-assembling biphenylpropyl ether (BpPr) dendrons were reported. It was demonstrated that similar mechanisms of self-assembly to those of other aryl ether dendrons persist, resulting in larger supramolecular dendrimers that pack into 2-D columnar lattices, 3-D cubic lattices, and 3D noncubic lattice and quasi-periodic arrays. Synthesis and retrostructural analysis of libraries of BpPr dendrons allowed for the discovery of new self-assembled

structures, including a banana-like lamellar crystal with a four layer repeat and extremely large vesicular interdigitated spheres. The interdigitated vesicular spheres formed from 770 *quasi-equivalent* dendritic building blocks exhibit ultrahigh molecular weight for supramolecular spheres,  $1.73 \times 10^6$  g/mol, and are among the largest monodisperse supramolecular objects observed, rivaled only by complex biological assemblies such as the ribosome. Vesicular spheres may provide more rapid access to larger spherical assemblies of interest for optoelectronic applications and the synthesis of monodisperse ultrahigh molecular weight polymers via a self-interruption of the polymerization process. An inverse relationship between the degree of branching of the dendron and the size of the corresponding supramolecular sphere was determined, and through the enhancement of size a continuum between small filled spheres and large hollow spheres was demonstrated. The synthesis of BpPr dendrons like most previous libraries has followed a generational approach, wherein a lower generation dendron is sequentially alkylated onto a repeated apex branching unit to provide higher generation dendrons with greater degrees of branching. Thus new approaches to dendron design aimed at minimizing the number of branches while retaining the desired supramolecular shape may result in structures of even larger size. Qualitative and quantitative comparisons of BpPr dendrons to previously reported libraries of benzyl, phenylpropyl, and biphenyl-4-methyl ether dendrons revealed that the shape of a supramolecular dendrimer, and also to an extent the self-organized lattice, is determined almost exclusively through the primary structure (branching sequence) of the dendrons. Like proteins, the primary structure of dendrons determines their tertiary structure. A 'nanoperiodic table' of self-assembling aryl ether dendrons was constructed, and through this table the primary structure of supramolecular dendron can therefore be used to predict their tertiary structure. Through this power of prediction, a retrosynthetic route to self-organized supramolecular dendrimers is accessible that may be able to replace in some cases the library approach to molecular design. Finally, this report demonstrates that the use of the library approach to discovery<sup>4b,c,18</sup> may be applicable to prediction.

**Acknowledgment.** Financial support by the National Science Foundation (DMR-0548559 and DMR-0520020) and the P. Roy Vagelos Chair at Penn are gratefully acknowledged. B.M.R. gratefully acknowledges funding from an NSF Graduate Research Fellowship and ACS Division of Organic Chemistry Graduate Fellowship (Roche).

**Supporting Information Available:** Experimental procedures with complete, spectral, structural, and retrostructural analysis. This material is available free of charge via the Internet at <http://pubs.acs.org>.

JA907882N

(40) Creighton, T. E. *Proteins: Structures and Molecular Properties*, 2nd ed.; W. H. Freeman: New York, 1992.

(41) (a) Seebach, D.; Overhand, M.; Kühnle, F. N. M.; Martinoni, B.; Oberer, L.; Hommel, U.; Widmer, H. *Helv. Chim. Acta* **1996**, *79*, 913–941. (b) Apella, D. H.; Christianson, L. A.; Karle, I. L.; Powell, D. R.; Gellman, S. H. *J. Am. Chem. Soc.* **1996**, *118*, 13071–13072. (c) Seebach, D.; Matthews, J. L. *Chem. Commun.* **1997**, 2015–2022. (d) Apella, D. H.; Christianson, L. A.; Klein, D. A.; Powell, D. R.; Huang, X.; Barchi, J. J.; Gellman, S. H. *Nature* **1997**, *387*, 381–384. (e) Gellman, S. H. *Acc. Chem. Res.* **1998**, *31*, 173–180. (f) Cheng, R. P.; Gellman, S. H.; Degrado, W. F. *Chem. Rev.* **2001**, *101*, 3219–3232. (g) Hill, D. J.; Mio, M. J.; Prince, R. B.; Hughes, T. S.; Moore, J. S. *Chem. Rev.* **2001**, *101*, 3893–4011. (h) Seebach, D.; Hook, D. F.; Glättli, A. *Biopolymers* **2006**, *84*, 23–37.